SEA SURFACE TEMPERATURE (SLSTR)

Algorithm Theoretical Basis Document

Title: Sea surface temperature (SLSTR) Algorithm
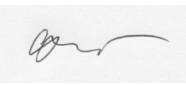
Theoretical Basis document

Document Number: SLSTR-ATBD-L2SST

Issue: 1

Revision: 2.5

Date: October 2012

Signature Table

	Name	Function	Company	Signature	Date
Prepared	C Merchant	Reader	University of Edinburgh		19 June 2010
Approved					

University of Edinburgh	SENTINEL-3 L2 PRODUCTS AND ALGORITHM DEFINITION	Document Ref: SLSTR-ATBD-L2SST-v2.5 Issue: 1 Date: October 2012

Released					

Document Change Record

Version	Date	Author	Description
2.0	8 April 2010	CJM	
2.1	5 May 2010	CJM	
2.2	19 May 2010	CJM	
2.3	23 Mar 2012	CJM	
2.4	26 Sept 2012	CJM & S MacCallum	
2.5	12 Oct 2012	CJM & S MacCallum	

From 2.0 To 2.1

Page	Section	Comments
3		Addition of document change record and distribution
39	Table 11	"A2" (meaning, across-track view two channel) changed to "N2" (adopted nomenclature).
	3	Reformat several equations to remove glitches in presentation; not content changes.
From 2.1 to 2.2		
32	Eq 3.18	Equation restored after inadvertent deletion
32 – 42		Equation number sequence corrected
From 2.2 to 2.3		
33	Table 9	Coefficients provided for N3R algorithm
36	Eq. 3.23	Inserted [2] previously omitted from equation in

From 2.3 to 2.4		definition of variance.
8	1.2	List of notations and parameters added
48	Sections 5, 6 and 7	Addition of level 1 section headings on validation, uncertainty budget and evolution.
48-51	8. References	Published references updated.
27	Eq. 3.4	Equation corrected
From 2.4 to 2.5		
32	Table 5	Viewing angles updated

Distribution:

Organisation	Name
ESA	Philippe Goryl, Alessandra Buongiorno and Carla Santella
EUMETSAT	Vincent Fournier-Sicre and Vincenzo Santacesaria
Consortium Partners	ARGANS, ACRI-ST, RAL, Brockmann-Consult, Elsag-Datamat

University of Edinburgh	SENTINEL-3 L2 PRODUCTS AND ALGORITHM DEFINITION	Document Ref: SLSTR-ATBD-L2SST-v2.5 Issue: 1 Date: October 2012

Table of Contents

University of Edinburgh	SENTINEL-3 L2 PRODUCTS AND ALGORITHM DEFINITION	Document Ref: SLSTR-ATBD-L2SST-v2.5 Issue: 1 Date: October 2012

List of Figures

1. INTRODUCTION

1.1 Acronyms and Abbreviations

ARC   ATSR Reprocessing for Climate

BT   Brightness Temperature

DISORT   Discrete Ordinates Radiative Transfer Program for a Multi-Layered Plane-Parallel Medium

GADS   Global Aerosol Data Set

LBL   Line-by-line

L2P   Level 2 pre-processed

NE$\square$T   Noise Equivalent Delta Temperature

NWP   Numerical Weather Prediction

RFM   Reference Forward Model

RMSD   Root-Mean-Square Deviation

RT   Radiative Transfer

RTE   Radiative Transfer Equation

RTM   Radiative Transfer Model

SD   Standard Deviation

SLSTR   Sea and Land Surface Temperature Radiometer

SRF   Spectral Response Function

SST   Sea Surface Temperature

TCWV   *Total Column Water Vapour*

ToA   *Top of Atmosphere*

University of Edinburgh	SENTINEL-3 L2 PRODUCTS AND ALGORITHM DEFINITION	Document Ref: SLSTR-ATBD-L2SST-v2.5 Issue: 1 Date: October 2012

8

1.2 Notation and Parameters

Retrieval parameters

$\mathbf{x}$	State vector (SST, humidity and temperature profile)
x	SST (element within state vector)
$\hat{x}$	SST estimate from retrieval
$\mathbf{y}$	Observation vector
F	Forward model function (simulation of $\mathbf{y}$ from $\mathbf{x}$)
$\mathbf{b}$	Forward model parameters
a_0	Offset coefficient
$\mathbf{a}$	Vector of weighting coefficients for observation vector
$\mathbf{S}_{yy}$	Covariance matrix of observations
$\mathbf{S}_\varepsilon$	Covariance matrix for noise equivalent differential temperature
$\mathbf{s}_{xy}$	Covariance vector of SST and observations
$\mathbf{k}$	Vector of modes of variation for the aerosol type
δ	Aerosol optical depth
c	Aerosol constant term
$\mathbf{K}$	Matrix of aerosol mode vectors, $\mathbf{k}$
N2	Across-track single-view 2-channel retrieval
N3	Across-track single-view 3-channel retrieval
D2	Dual-view 2-channel retrieval
D3	Dual-view 3-channel retrieval

Radiative transfer modelling parameters

L	Intensity of radiation

τ	Optical depth (may appear with subscript i to indicate different aerosol components)
μ	Cosine of the zenith angle θ
θ	Zenith angle
ω	Single scattering albedo (may appear with subscript i to indicate different aerosol components)
B	Planck radiance
T	Temperature
P	Single-scattering phase function (may appear with subscript i to indicate different aerosol components)
λ	Wavelength
z	Height
h	Scale height (km)
N	Aerosol concentration at the surface (0) and at height (z)
SST	Skin temperature for profile
T_0	Temperature of ice-free conditions (2 °C)
T_1	Temperature of ice-covered conditions (-1.8 °C)
ice	Sea ice coverage (fractional)
$n_{1,2}$	Random variables sampled from a Poisson distribution with a mean of 5

Uncertainty modelling parameters

ε_F	Radiative transfer model error
ε_x	Errors due to systematic differences between state vectors and reality
ε_b	Errors in model parameters
ε_y	Forward model error (combination of ε_F, ε_x, and ε_b)
$\mathbf{y}_p$	Simulated BTs after perturbation, Δb, of parameter b, of the forward model
$\mathbf{e}_b$	Error in BT from parameter error of size Δb

$\mathbf{e}_{SST}$ Error in SST from parameter error of size Δb

ε_{rad} Radiometric noise (overall)

ε_{1-n} Radiometric noise (for channel/view combinations 1 to n)

$\varepsilon_{PR-symmetric}$ Symmetric pseudo-random error

$\varepsilon_{PR-asymmetric}$ Asymmetric pseudo-random error

n_c Number of clear pixels (in a 3x3 box)

$\varepsilon_{totalrandom}$ Total (pseudo) random error (combination of ε_{rad}, $\varepsilon_{PR-symmetric}$, and $\varepsilon_{PR-asymmetric}$)

w Prior estimate of total column water vapour

m Gradient of $\varepsilon_{PR-symmetric}$ as a function of TCWV (retrieval-type specific)

C Offset for $\varepsilon_{PR-symmetric}$ as a function of TCWV (retrieval-type specific)

Grid Cell Averaging / Atmospheric Smoothing

k,l Pixel coordinates

i,j Cell coordinates

$G_{k,l}$ Cloud screening operator for pixel, *k,l*, for grid cell averaging

$\varepsilon_{i,j}$ Error for grid cell *i,j*

$V_{SST,i,j}$ Variance of SSTs in the cell, *i,j*

G_p Atmospheric smoothing operator for index *p* of 3x3 pixel box

$\varepsilon_{rad-L2P}$ Radiometric error in L2P SST

e Particular realisation of an error drawn from and error distribution of standard deviation, ε

$\varepsilon_{L2P-SSES}$ Total error in L2P SST (combination of $\varepsilon_{rad-L2P}$ and pseudo-random errors)

1.3 Purpose and Scope

To describe the physical and statistical basis for estimation of sea surface temperature (SST) and associated errors in SST, for products of the SLSTR.

1.4 Algorithm Identification

Sea surface temperature and error estimate, per ocean pixel, in gridded products, and in L2P products.

2. ALGORITHM OVERVIEW

2.1 Objectives

The objectives of the algorithms defined herein are: to estimate the sea surface temperature and give an associated error estimate using combinations of brightness temperatures weighted by coefficients. The coefficients are to be based on physical modelling (to be independent of in situ observations), followed by regression to an equation whose form accounts for view-geometric and other factors, to give a minimum variance SST estimate. Different combinations of coefficients are required for different circumstances, and these are described.

3. ALGORITHM DESCRIPTION

3.1 Theoretical Description

3.1.1 Specification of the Forward Model

3.1.1.1 Introduction

Coefficients for SST retrieval can be defined using radiative transfer (RT) modelled radiances, and must be derived in this way if independence from in situ observations is required, as for SLSTR. Figure 1, from Merchant and Le Borgne (2004), provides a schematic illustration of the process. Defining the coefficients requires the radiances observed by the infrared sensor, as it views the ocean, to be simulated for realistic clear-sky conditions. The complete setup for performing this simulation is defined as the "forward model" and consists of a number of elements, of which one is the software to simulate the radiances – the radiative transfer model (RTM). Other significant components of the forward model include spectroscopic data, sensor characteristics, and a representative set of states on which to perform the simulations. The following sub-sections describe the components of the forward model further and define some minimum requirements for forward modelling required for SLSTR.
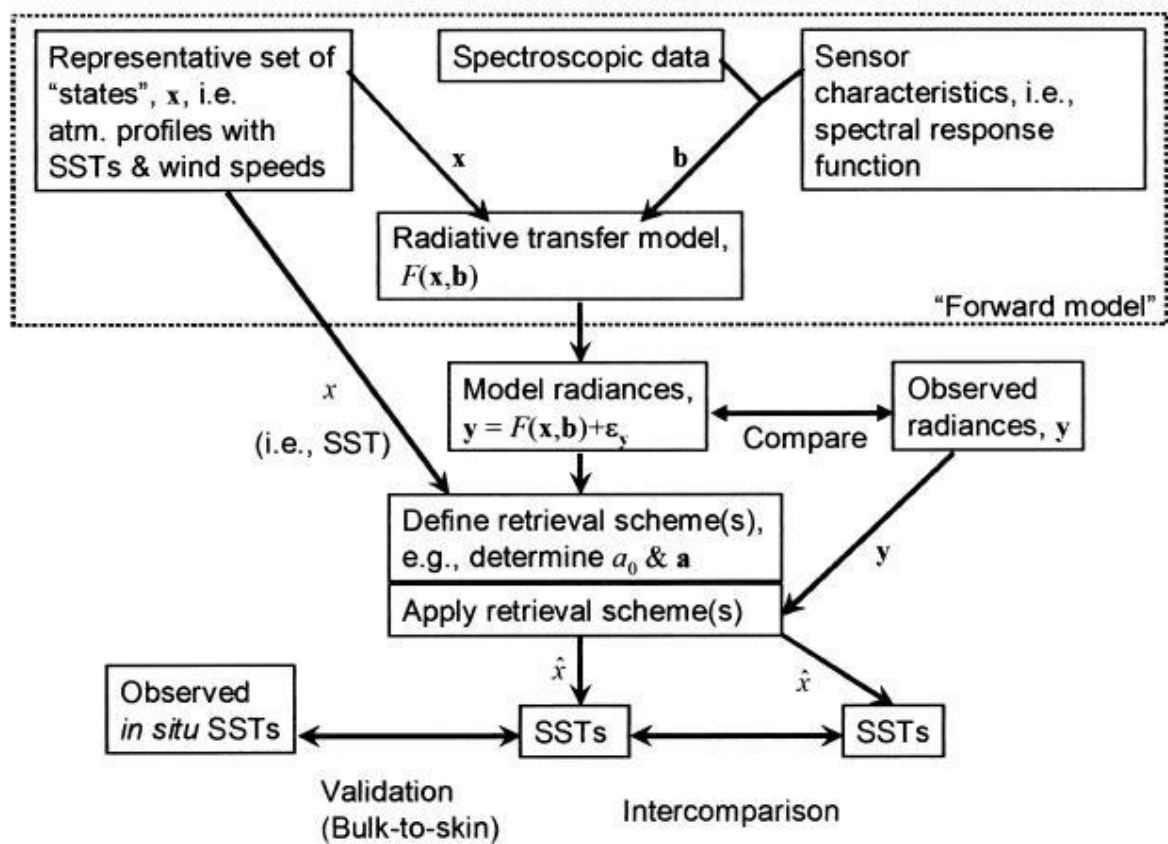
Figure 1. Schematic of the process of defining and validating coefficients for sea surface temperature retrieval using radiative transfer modelling, from Merchant and Le Borgne (2004).

Radiative transfer model

Radiative transfer models (RTMs) are used to model the passage of radiation through a medium, such as the Earth's atmosphere. There are three main processes performed by a RTM. Firstly the optical properties of the medium must be determined from its physical properties, such as composition, pressure, and temperature. Secondly boundary conditions must be chosen. Finally the radiative transfer equation must be solved. For satellite remote sensing, RTMs are used to predict the radiances observed by a satellite given the surface temperature, surface emissivity, and profiles of atmospheric pressure, temperature and gas concentrations.

A very accurate RTM is required for the derivation of SST retrieval coefficients. To achieve the necessary accuracy a line-by-line (LBL) transmittance model is required. The effects of tropospheric and stratospheric aerosols, and radiatively active gases must be simulated. Due to aerosol particles having radii comparable to the wavelengths of thermal infra-red radiation, it is necessary to use a RTM which includes the effects of scattering – such as "DISORT" (Stamnes, Tsay, Wiscombe and Jayaweera, 1988).

13

In addition to the RTM it is also necessary to specify several associated datasets and models. These include the spectral response functions (SRFs) of the instruments, atmospheric profiles to be used for the simulations, distributions of gases which have a significant impact on the observed radiances, and single scattering properties of the aerosols. A surface emissivity model is also required to calculate the surface emissivity given the sea surface state (temperature, wind speed, viewing angle etc.).

Line-by-Line model

Line-by-line radiative transfer models determine the optical properties of the atmosphere to a very high accuracy through detailed treatment of the interaction between radiation and gas molecules. All calculations are monochromatic – at a single frequency / wavelength – and account for individual absorption lines modified by effects such as pressure and Doppler broadening. This allows the transmission and hence the radiance to be modelled at any spectral resolution required.

Spectroscopic database

Radiative transfer calculations in the RTM are based on spectroscopic parameters for the relevant atmospheric species (gases and aerosols). A spectroscopic database contains a list of all known absorption lines, their central frequency and strength. Depending on the RTM, these spectroscopic parameters may be explicit, separated from the software, or implicit, embedded in it. As new measurements are made, the databases should be updated allowing line-by-line models to make use of the updated spectroscopy. An RTM linked with an external spectroscopic database is recommended to ensure up to date spectroscopy is used. One example of such an RTM is the Reference Forward Model (RFM), which uses the HITRAN spectroscopic database.

RTM simulations in the definition of retrieval coefficients

Linear and near-linear retrieval schemes are nearly optimal for SST estimation if the infrared radiances are expressed as brightness temperatures (BTs). As such, the SST retrieval coefficients are defined using RTM-simulated BTs. Typically, BTs are defined in units of kelvin (K) and consequently accuracies associated with SST retrievals are defined in K in this document.

3.1.1.2 Requirements for clear sky radiative transfer

The RTM to be used for defining SST coefficients must meet the criteria detailed in this subsection. The most fundamental of these criteria is the accuracy of the simulated radiances. Merchant and Le Borgne (2004) propose that overall, a forward model should be capable of simulating the differences in BTs arising from different clear-sky states, to an accuracy (bias)

of ~0.1 K. This equates to the minimum level of accuracy desired in infrared sensors used for SST retrievals. This minimum accuracy requirement refers to the forward model and not merely the RTM component (i.e. it accounts for sensitivity of the RTM to uncertain parameters such as trace gas and water vapour profiles).

These criteria are intended to ensure that the RTM is capable of simulating the differences in BTs arising from different clear-sky states, to an accuracy (bias) of ~0.1 K. In order to attain the minimum accuracy requirement of the forward model as a whole, the forward modelling simulations:

Should be capable of simulating radiances at a spectral resolution of 0.01 cm^{-1} or better.

Should include CO_2 line mixing. As a minimum requirement, the RTM must include first order line coupling in the Q branch (e.g. Tobin and Strow, 1994). Second order line coupling for the Q branch and first order line coupling for the P and R branches should by preference be included but are less critical.

Must be able to model continuum-like features associated with particular molecules. In particular continuum absorption must be considered for water vapour and N_2.

Should be calculated with the assumptions that the Planck function varies linearly with altitude and the optical depth varies linearly with path within each layer. An algorithm for linearity with path within each layer ('linear-in-tau' approximation) is described by Clough et al (1992). This method more accurately models the radiance from optically thick atmospheric layers.

Should use linear interpolation for profiles of absorber quantities. Linear interpolation is preferred over logarithmic interpolation as some trace gas quantities may be near-zero at certain altitudes.

Should use Voigt line shapes with a chi correction to define spectral line shapes for CO_2, in order to include an appropriate correction to the sub-Lorentzian CO_2 absorption wings, affecting spectra around 4.1 to 4.2 μm. Voigt line shapes may be used for all other molecules.

Must include all trace gases that have an impact of >0.001 K on ToA BTs, for any channel. For example, the following gases are be represented in the RTM for generating SST coefficients in the ARC project (Merchant et al, 2008): H_2O, CO_2, O_3, N_2O, CH_4, NH_3, HNO_3, OCS, H_2CO, N_2, C_2H_6, F11, F12, F22, F113, F114, CCl_4, HNO_4. This list may depend on the instrumental channels and assumed trace gas profiles appropriate to the instrument and epoch, but is likely to be the same for SLSTR.

Should use water vapour spectroscopy based on the water vapour continuum absorption parameterization, MT_CKD (Clough, 2002, personal communication), or subsequent developments thereof, consistent with the treatment of the far wings of spectral lines in the RTM and spectroscopic database.

Should use a spectroscopic database such as HITRAN 2000 (with updates) or later, provided it is consistent with the continuum absorption parameterisation.

The Reference Forward Model (RFM) fits these requirements and has been used in the ARC project (Merchant et al, 2008). An example of an RFM input script, showing non-default settings required to meet the criteria above, is given in Listing 1.

```
!Driver file generated by rfm.py
*HDR
   RFM - ATBD example
*FLG
   NAD MIX CTM SFC RAD BFX LIN SHP
*SPC
   BandA 650.00 1250.0 0.01
   BandB 2150.0 3450.0 0.01
*GAS
   h2o co2 o3 n2o ch4 n2(CTM), nh3, hno3, ocs, h2co, c2h6, f11, f22, f113, f114,
ccl4, hno4
*ATM
   /disk/scratch/local/atm/lbl6.atm
   /disk/scratch/local/atm/minor.atm
*SEC
   1.00
*SFC
   288.0 1.00
*HIT
   /disk/scratch/local/HITRAN/tes.bin.nag
*END
```

Spectral response functions

The ESA approved SRFs will be used, linearly interpolated to the spectral resolution of the simulations.

3.1.1.3 Spectral Emissivity Model

Values of the infrared emissivity of water surfaces are another important component of the forward model, and require a spectral emissivity model to calculate them. Such a model must account for the emissivity variations associated with wavelength, view angle, wind speed and water temperature. The emissivity effect of variability in ocean salinity may be neglected. A suitable emissivity model is described by Embury et al. (2009).

Embury et al. (2009) (hereafter E2009) model the emissivity at any view angle using the following methods. They assume the sea surface consisting of plane facets with a wind speed dependent slope distribution, calculate Fresnel reflection coefficients for each facet, and obtain the sum of their contributions (Masuda et al, 1988 and Masuda, 2006). In addition to the direct emission, E2009 also include a contribution from emitted radiation that has been reflected by the surface into the view angle (Watts et al. 1996, Wu and Smith 1997).

The isotropic Gaussian version of the clean surface slope distribution measured/modelled by Cox and Munk (1954) provides an appropriate description of the sea slope distribution (i.e., wind azimuth

angle need not be considered). This distribution also provides an estimate of the background mean squared slope due to swell.

In order to avoid significant errors in simulated BTs the emissivity model must account for the temperature dependence of emissivity (Newman et al. 2005). This may be achieved through the use of temperature dependent values of refractive indices of water (pure and sea water). The refractive indices of Newman et al (2005) are recommended for the frequency range 760-1230 cm^{-1}, and those of Downing et al (1975) elsewhere. Suitable treatment of the temperature dependence of the refractive indices is given by Newman et al (2005) for the range 760-1230 cm^{-1}, and by Pinkley et al (1977) for other spectral regions. Temperature and salinity dependences may be assumed independent, and may be combined to calculate refractive indices for sea water (using a fixed standard value of 35 PSU) at different temperatures.

It is not necessary for the emissivity model to include the effect of sea surface foam, which will affect the emissivity at higher wind speeds. The effect of foam on the emissivity is likely to be smaller than the maximum effect proposed in Watts et al (1996), demonstrated by Salisbury et al (1993) who show emissivity is unaffected by foam in the 8-14 µm region. In addition, the temperature of the foam may not match the skin temperature (Marmorino, 2005).

3.1.1.4 Requirements for simulation of scattering

The monochromatic radiative transfer equation assuming a plane-parallel atmosphere and azimuth independence is:

$$\mu \frac{dL(\tau,\mu)}{d\tau} = L(\tau,\mu) - (1-\omega)B(T) - \frac{\omega}{2}\int_{-1}^{+1} L(\tau,\mu')P(\mu,\mu')d\mu' \qquad 3.1$$

where L is the intensity of radiation at optical depth τ and μ (cosine of the zenith angle θ), ω is the single scattering albedo, B(T) is the Planck radiance at temperature T (which is itself a function of the height variable – optical depth in this case), and P is the single-scattering phase function.

When scattering can be ignored (i.e. ω=0) the above equation can be significantly simplified and can be solved analytically under certain conditions. This is done for the line-by-line gas transmittance models and fast models.

Whether absorption or scattering is dominant depends on the size of the particles compared to the wavelength of the radiation. If the particles are much smaller than a wavelength then absorption dominates. But when the particle size is comparable to the wavelength, the radiation can be scattered and the full radiative transfer equation must be considered.

For the case of infra red radiation passing through the atmosphere the majority of particles are gas molecules which are much smaller than infra-red wavelengths – hence the absorption only approximation used in line-by-line and fast models. However aerosol particles (both marine and stratospheric) have radii comparable to λ_{IR} so we require a scattering model to investigate the effects due to aerosols.

Scattering code

A highly accurate method of solving the radiative transfer equation (RTE) for plane-parallel problems (where optical properties are one dimensional – i.e. a function of z only) is required. Transmission profiles from the LBL model can be used to solve the RTE. Monochromatic transmission spectra can be convolved with the instrument SRFs to give channel integrated transmissions, which can then be used to calculate aerosol delta-BTs using the scattering model. The BT differences are then added to clear-sky BTs, calculated by integrating the ToA radiance spectra from the LBL model. An example of a suitable scattering model is the discrete ordinates (DISORT) radiative transfer model. It has been extensively tested and was chosen as the reference scattering model in the ARC project (Merchant et al, 2008).

Scattering properties

In addition to the RTE solver it is also necessary to know the optical properties of the various aerosols (marine, stratospheric etc) and combine them with the optical properties of the clear-sky atmosphere. The properties that must be used in the scattering code are as follows: the optical depth, single scattering albedo, and phase function. The properties of several different components can be combined using:

$$\tau = \sum \tau_i$$

$$\omega = \frac{\sum \omega_i \tau_i}{\tau}$$

$$P(\Theta) = \frac{\sum P_i(\Theta)\omega_i \tau_i}{\sum \omega_i \tau_i}$$

3.2

Where the subscript *i* indicates the different aerosol components used. For the clear-sky component the single scattering albedo is zero, i.e. no scattering, and the phase function is unity (the actual value does not matter as it will be weighted by the single scattering albedo).

Optical properties of marine aerosols shall be obtained from an appropriate database, such as the Optical Properties of Aerosols and Clouds (OPAC) database. The chosen dataset should include both microphysical and optical properties (the latter calculated from the former using Mie theory) for different aerosol components, such as those given in Table 1. These basic components can be combined to represent the various mixtures observed in the atmosphere (i.e. maritime, continental etc).

Component	Description	RH Dependent
Insoluble	Soil particles and organic material	N
Water-soluble	Sulphates, nitrates and water-soluble organics	Y
Soot	Black carbon particles	N

Sea salt (acc. mode)	Salt from seawater (fine particles)	Y
Sea salt (coa. mode)	Salt from seawater (large particles)	N
Mineral (nuc. mode)	Desert dust (very fine particles)	N
Mineral (acc. mode)	Desert dust (fine particles)	N
Mineral (coa. mode)	Desert dust (large particles)	N
Mineral-transported	Desert dust after extended time in atmosphere	N
Sulphate droplets	Sulphate in Antarctic aerosol (no nitrates etc)	Y

Table 1. Example of marine aerosol components that should be included in the database (e.g. OPAC) used for simulating aerosol scattering.

Optical properties for stratospheric sulphate aerosol must also be considered. These may be calculated using Mie scattering theory and H_2SO_4 refractive index data (Tisdale et al,1998) assuming a lognormal size distribution. Information about size distributions representative of various states of stratospheric aerosol is given in Deshler et al (2003).

Finally, optical properties of Saharan dust from Highwood et al. (2003) are recommended in preference to the OPAC mineral-transported component. Highwood et al. used AERONET observations from Dakhla to derive the aerosol optical properties. These parameters have been found to match observations more closely than the OPAC mineral-transported component (Merchant et al, 2006).

3.1.1.5 Atmospheric Profile Sets

A representative distribution of ToA BTs, simulated using an RTM, is required to define the retrieval coefficients. In order to obtain such a distribution of simulated ToA BTs, it is necessary to have a representative distribution of atmospheric states – i.e. profiles of atmospheric temperature, water vapour and associated surface variables. There are two distinct sources of this type of data: measurements in the form of radiosondes, and simulated data from numerical weather prediction (NWP) models.

NWP data should be used in preference to radiosonde data for generation of SST retrieval coefficients (Merchant 99), as these avoid the problems inherent in radiosondes – data are available for the entire globe and all required surface and atmospheric fields are available for each data point. Any NWP model biases will be included in the dataset and can influence the resulting SST retrieval coefficients, but the same is true for radiosonde data sets.

A dataset containing representative set of profiles (of the order 10^3 profiles) should be constructed by sampling and filtering data from a larger NWP database. The source database must contain both surface parameters and profiles of temperature and relative humidity. An example of a suitable source data set is the ERA-40 database, as used in the ARC project (Merchant et al 2008). This consists of 6-hourly, surface and profile (on 60 pressure levels), NWP data from 1957-2001, on a 2.5° horizontal grid. Such a large data source is not required and basic temporal sampling should be applied to reduce the size of the dataset. This initial

sampling should leave a subset of data covering all times of day for all seasons. For example, the initial stage of the construction of the 60L-SD data set (Chevallier, 2001), used as the starting point for the ARC project database, is to extract a subset of data from the ERA-40 dataset: days 1 and 15 of every month in 1992 and 1993 (approximately seven million profiles).

The second step in the construction of the 60L-SD dataset is to further sample the data to remove bias towards a particular atmospheric state, while maintaining the full range of possible atmospheric variability. This is achieved through an iterative sampling strategy (Chevallier, 2001), where profiles are selected randomly but only kept if they are sufficiently different from previously extracted profiles (in terms of temperature, water vapour and ozone), rather than through a fixed spatial-temporal sampling strategy.

The final 60L-SD dataset used in the ARC project (Merchant et al, 2008) contains 13,495 profiles. Further filtering of this dataset is required to provide a final dataset suitable for generating SST retrieval coefficients. It is recommended that all profiles meeting the following criteria are removed.

All land or mixed land/ocean profiles

All profiles with >95% sea ice

All profiles outside RTTOV water vapour range (Saunders and Brunel, 2005) given in Table 2

All profiles with >95% relative humidity for any layer (cloudiness increases as area-average RH rises above 70% simulations, and such profiles therefore represent conditions of near-total cloud cover, not representative of the locations of SST retrieval)

Any profiles that cause the RTM to crash, provided these are a small fraction (< 2%) of all profiles run.

While the sampling strategy outlined above and by Chevallier (2001) provides a good representation of the sampled variables (temperature, water vapour, and ozone) it does not necessarily represent variability in other variables well. In particular, trace gases affect the observed BTs and are strongly dependent on latitude/season. A uniform distribution over latitude and season is the simplest acceptable way in which to represent variability in trace gases. In order to achieve this without losing the benefit of the 60L-SD sampling strategy, it is recommended that a uniformly distributed profile set is constructed by combining the original dataset (e.g. 60L-SD) with profiles taken from a larger pool of NWP profiles. Additional profiles should only be added where the original dataset does not contain a sufficient number of profiles in the given latitude/month bin. The recommended geographical

sampling strategy for this filling step is to have a minimum of 16 profiles in each time-latitude domain of size 1 month by 15 degree latitude with an spread of longitudes within each domain. Note that there is no precise method for specifying the size and sampling strategy for the profile set for radiative transfer modelling, and the recommendations above are "safe" in that they are known to work well from experience in ARC.

Pressure	Min. Water Vapour (kg/kg)	Max. Water Vapour (kg/kg)
0.10	2.479E-06	3.649E-05
0.29	2.479E-06	3.877E-05
0.69	2.479E-06	3.841E-05
1.42	2.479E-06	3.761E-05
2.61	2.479E-06	3.571E-05
4.41	2.479E-06	3.547E-05
6.95	2.479E-06	3.635E-05
10.37	2.479E-06	3.627E-05
14.81	2.479E-06	3.339E-05
20.40	2.479E-06	3.357E-05
27.26	2.479E-06	3.479E-05
35.51	2.479E-06	3.018E-05
45.29	2.479E-06	2.857E-05
56.73	2.479E-06	2.772E-05
69.97	2.479E-06	2.695E-05
85.18	2.479E-06	2.504E-05
102.05	2.479E-06	2.419E-05
122.04	2.479E-06	2.979E-05
143.84	2.479E-06	7.176E-05
167.95	2.479E-06	1.369E-03
194.36	2.479E-06	2.322E-03
222.94	2.479E-06	3.696E-03
253.71	2.479E-06	6.370E-03
286.60	2.479E-06	9.307E-03
321.50	2.479E-06	1.401E-02
358.28	2.479E-06	2.119E-02
396.81	2.479E-06	3.019E-02
436.95	2.479E-06	4.168E-02
478.54	2.434E-06	5.419E-02
521.46	5.635E-06	6.461E-02
565.54	1.301E-05	7.458E-02
610.60	1.617E-05	8.783E-02
656.43	1.780E-05	1.033E-01
702.73	2.133E-05	1.175E-01
749.12	4.537E-05	1.323E-01
795.09	6.679E-05	1.479E-01
839.95	8.028E-05	1.663E-01
882.80	8.350E-05	1.781E-01
922.46	8.209E-05	2.002E-01
957.44	8.209E-05	2.247E-01
985.88	8.209E-05	2.324E-01
1005.43	8.209E-05	2.350E-01
1013.25	8.209E-05	2.365E-01

Table 2. Recommended minimum and maximum limits for water vapour profiles to be used in the profile data set for SST retrieval coefficient generation.

The skin temperature must be that relevant to the ocean water part of any mixed cells. Where sea ice fraction is >0%, the water skin temperature needs to be estimated from the bottom boundary temperature of the profile (the 2 m air temperature) and an appropriate means of replacing it with a water temperature is given by Eq. 3.3 (Matthiesen and Merchant, 2003).

$$SST = T_0 + \frac{1 - ice}{T_0 - T_1} \frac{n_1}{5} + \frac{n_2}{5}$$

3.3

Where T_0=2 °C and T_1=-1.8 °C are end points of the interpolation representing ice-free and ice-covered conditions respectively; *ice* is the sea ice coverage (0 to 1); n_1 and n_2 are random variables sampled from a Poisson distribution with mean of 5. (This statistical approach is an improvement on the assumption sometimes made that water near sea-ice is necessarily close to freezing temperature.)

Trace gases

Trace gases also affect the observed BTs and are strongly dependent on latitude / season. For NWP only one atmospheric gas is relevant – water vapour – all other gases are simply considered to be 'air'. Water vapour is also the primary absorber of radiation in the atmosphere, and hence the most important gas to consider in radiative transfer simulations. However, as can be seen from Figure 2, other gases are still significant and cannot be neglected. Gases other than water vapour will be referred to as 'trace gases' – this includes nitrogen and oxygen, which although constituting the majority of the atmosphere, have relatively little impact on ToA BT in the relevant portion of the spectrum.
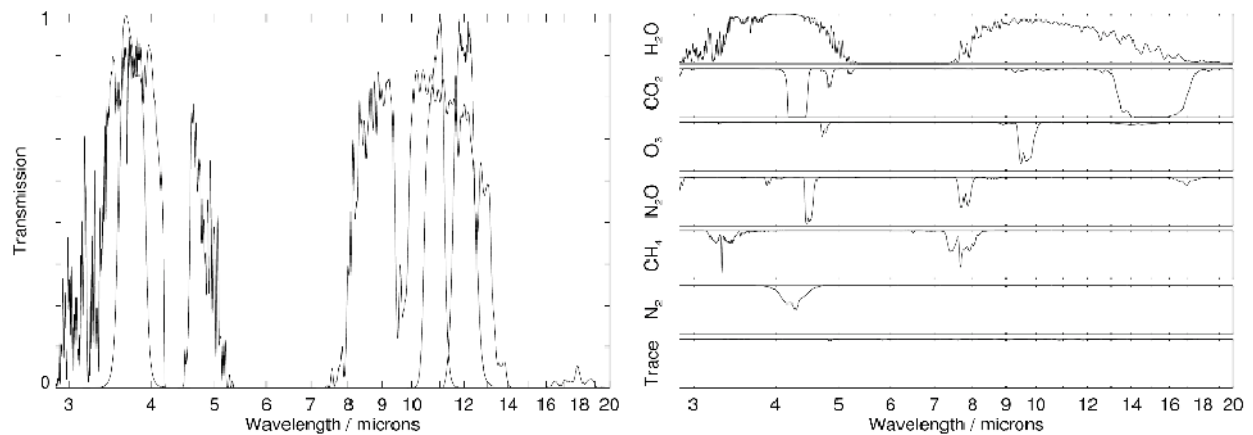
Figure 2. Left: Total atmospheric transmission mid-latitude day-time MIPAS model atmosphere, superimposed on ATSR thermal SRFs. Right: Transmission due to individual atmospheric absorbers. Trace refers to all other HITRAN gases.

The trace gases which have a significant effect on the ToA BTs can be determined through comparisons of RTM simulations for water vapour only and water vapour + trace gas atmospheres, for each of the gases in the spectroscopic database independently. All gases

which have an impact greater than 0.001 K in any channel should be included in RTM simulations.

Effects of geographic and seasonal variations in trace gas concentrations on ToA BTs should also be considered. This may be done through RTM simulations of model atmospheres for different locations/times. Again the threshold of 0.001 K should be used to determine whether the effect of geographic or temporal variations in trace gas concentrations are significant enough that they must be accounted for.

The gases whose geographic or temporal variations have a significant impact on AATSR ToA BTs are shown in Table 3 and are discussed below. Simple linear interpolation between model atmospheres at different locations/times is generally appropriate for these gases. Global profiles may be used for trace gases whose variations have negligible impact on ToA BTs. Trends in trace gases prevent the definition of appropriate profiles for SLSTR at this stage.

Gas	Long Term Trend	Annual Cycle	Latitudinal Variation
NH_4	Y	N	N
HNO_3	Y	Y	Y
N_2O	Y	N	Y
CH_4	Y	N	Y
CFC 11	Y	N	Y
CFC 12	Y	N	Y
CO_2	Y	N	N

Table 3. Gases for which geographical and temporal must be accounted for in RTM simulations for defining SST retrieval coefficients for AATSR.

HNO_3

Geographic variations of nitric acid (based on MIPAS model atmospheres) affect the AATSR 11 µm channel by ~0.2 K. Figure 3 shows HNO_3 climatology calculated from microwave limb sounder (MLS) data (Sentee et al, 2007). Variations in concentration from < 5ppbv at the equator to > 20 ppbv in polar-winter areas explain the large geographic variation in BT impact. Significant seasonal trends in HNO_3 at mid to high-latitudes are also shown in Figure 3. The best climatology available at time of coefficient derivation (such as an updated version of the data behind the right-hand panel in Figure 3) should be used.

Figure 3. Peak stratospheric HNO_3 concentrations recorded by the MLS instrument on-board AURA. Left: time series since August 2004. Right: seasonal climatology.

N_2O

Nitrous oxide variation has an effect ~0.036 K on the AATSR 3.7 µm channel. The MLS instrument also measures N_2O, the climatology from which is shown in Figure 4. There is significant geographic variation but seasonal variation is negligible, except at extremely high latitudes.
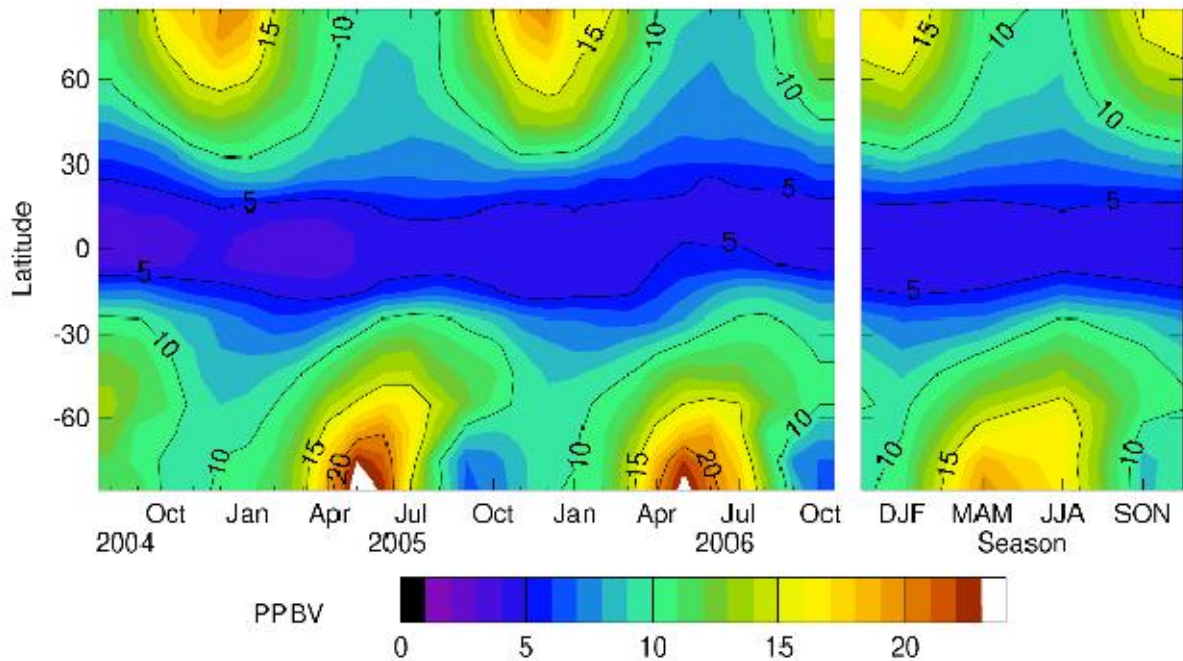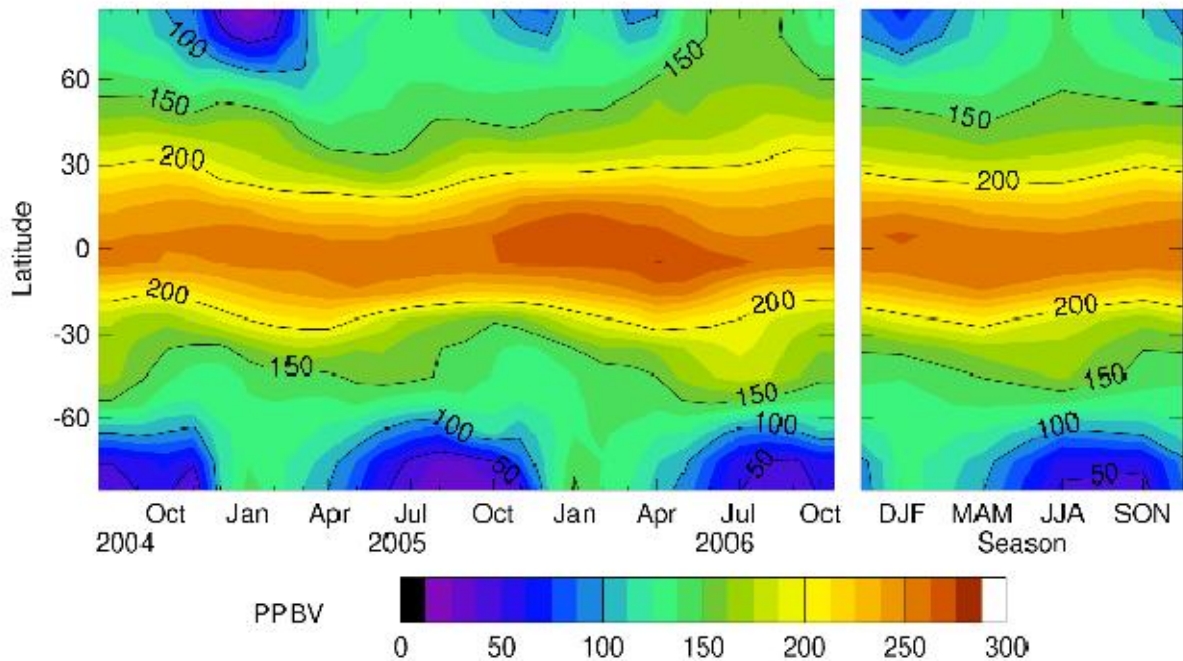
Figure 4. N_2O concentrations at 32 mbar recorded by the MLS instrument on-board AURA. Left: time series since August 2004. Right: seasonal climatology.

CH_4

Variability of the methane profile affects the AATSR 3.7 µm BT by 0.005 K. However, it is also correlated with the N_2O impact. Climatology of CH_4 from 1991 to 2002 is available from the Halogen Occultation Experiment (HALOE), which flew on board the Upper Atmosphere Research Satellite (UARS). As for N_2O, there is strong geographic variation but negligible seasonal variation.
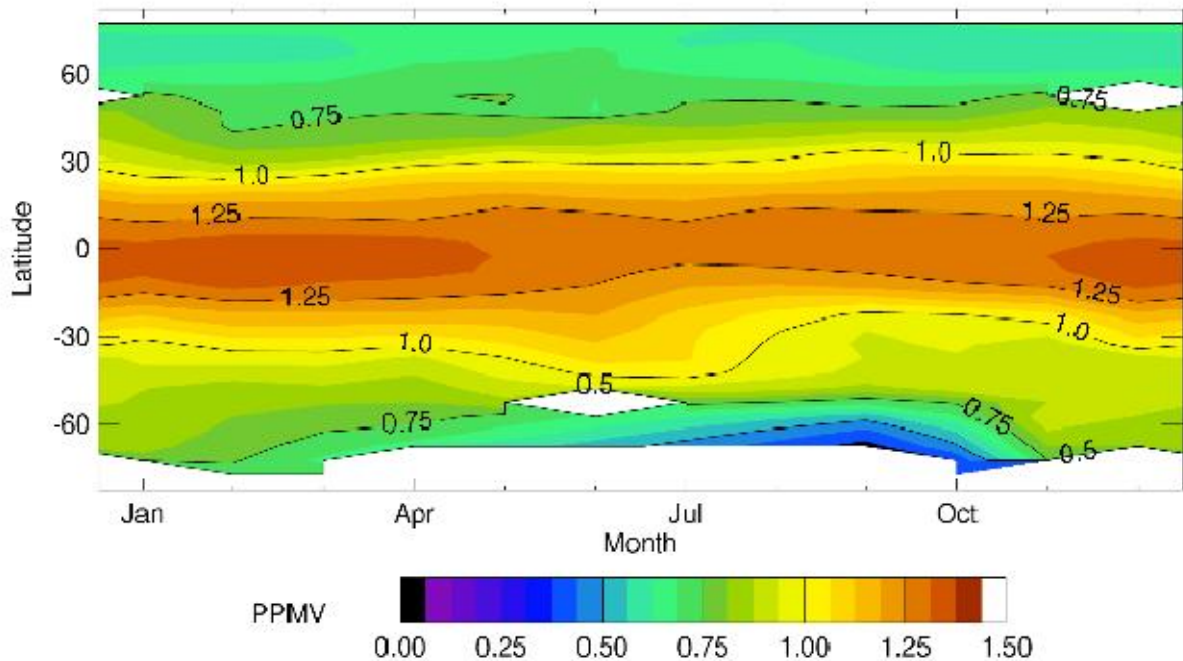
Figure 5. CH$_4$ concentrations at 10 mbar from the HALOE climatology of HALOE.

CFCs

Two chlorofluorocarbons (CFC-11 and CFC-12) absorb strongly in the long wavelength channels, with latitudinal variations of ~0.02 K observed for AATSR. Furthermore as the gases affect different channels (CFC-11 affects 12 µm, while CFC-12 affects 11 µm) split-window algorithms which depend on the difference between the two channels will be particularly sensitive.

Climatology for CFCs may be calculated from observations made by the Cryogenic Limb Array Etalon Spectrometer (CLAES) instrument on UARS. Figure 6 shows the climatology for CFC-11 and CFC-12 at 46 mbar, as calculated from CLAES observations. Strong latitudinal variation is observed but significant seasonal variation is not present below 60 degrees.

Figure 6. Climatology of CFC concentrations at 46 mbar derived from CLAES observations.

Long term trends

In addition to the geographic and seasonal variations in trace gases discussed above, there are also long term trends in trace gas concentration. During the course of the (A)ATSR missions, atmospheric concentrations of $CO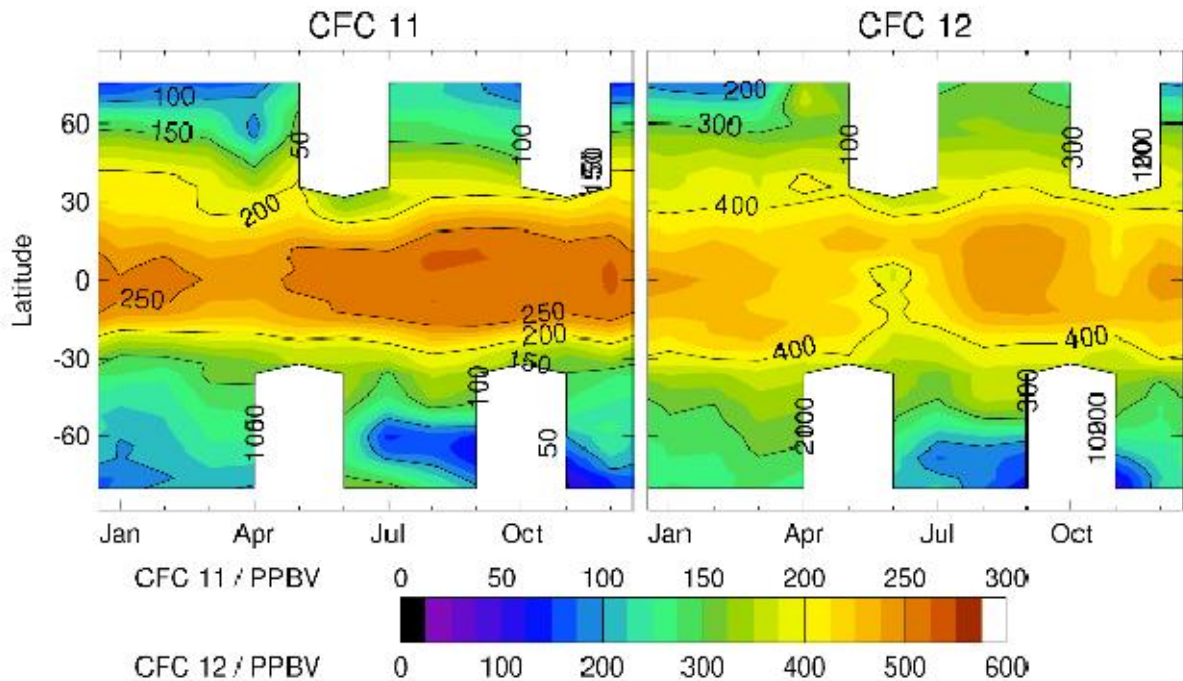_2$ have increased from ~355 ppmv to ~385 ppmv, equivalent to a change of ~0.015 K in the 11 µm and 12 µm BTs. This is negligible in terms of geographic or seasonal variation but it is significant as a long term trend where stability of < 0.05 K decade^{-1} is required. It is recommend that atmospheric CO_2 from the Carbon Dioxide Information Analysis Centre (CDIAC; Keeling and Whorf, 2005) at the Oak Ridge National Laboratory be used to scale the vertical distribution from the MIPAS model atmosphere to the appropriate annual concentration to derive coefficients for the year of SLSTR launch.

Changes in N_2O and CH_4 over the (A)ATSR lifetime are equivalent to a decrease of ~0.02 K in 3.7 µm BTs. Annual concentrations can be obtained from CDIAC (Blake, 2005) for methane, and the National Oceanic and Atmospheric Administration (NOAA) Climate Monitoring and Diagnostics Laboratory (CMDL) for nitrous oxide. Likewise, these should be used to rescale a standard atmospheric profile for these gases.

Concentrations of CFCs are also provided by CMDL. Their variation is equivalent to ~0.02 K but unlike the other trace gases considered here, the concentration of CFCs is no longer increasing.

Aerosol profiles

Tropospheric aerosols can be assumed to follow a simple exponential with height, given by:

$$N(z) = N(0)\exp(-z/h) \qquad\qquad 3.4$$

Where $N(O)$ is the aerosol concentration at the surface, and h is the scale height in kilometres. The OPAC dataset contains a set of aerosol profiles of this form. These aerosol profiles are associated with different geographical locations, and differ in terms of components present and surface concentrations. A climatology of aerosol conditions, such as the Global Aerosol Data Set (GADS), should be used alongside the optical propertied dataset (OPAC) to give a good representation of aerosol profiles.

For stratospheric aerosols that are present after major volcanic eruptions, in situ measurements of size distribution are available for a 30 year period at Laramie, Wyoming (Deshler et al, 2003). These data provide vertical profiles of both the number density and size distribution necessary to calculate aerosol optical properties using Mie theory. Single scattering properties should be calculated for the seven aerosol modes given in Table 4, and refractive index data from Tisdale et al, 1998 assuming a 75% concentration of H_2SO_4. Scattering properties can then be interpolated between the seven pre-calculated sets based on altitude.

Size Distribution	Median Radius	Distribution Width
OPAC Sulphate	0.0695	2.03
A (primary)	0.025	2.15
B (primary)	0.08	1.50
C (primary)	0.05	1.50
D (primary)	0.13	1.40
E (secondary)	0.35	1.20
F (secondary)	0.55	1.20
G (secondary)	0.75	1.20

Table 4. Recommended aerosol modes for calculating single scattering properties for stratospheric sulphate aerosols.

3.1.1.6 Procedural Flow of the Forward Model

The components of the forward model outlined in the previous subsections are combined together as follows.

Monochromatic radiance and transmission spectra are calculated using the line-by-line model with inputs taken from the emissivity model and atmospheric profile dataset. Convolution of the LBL model output with the instrument SRFs yields clear-sky BTs, and channel-integrated

transmission values. This channel-integrated data is then used, alongside the aerosol model data, as input to the scattering code (DISORT, in the ARC example), to provide aerosol BT differences.

3.1.2   Definition of the Retrieval Coefficients

3.1.2.1 SST retrieval and calculation of retrieval coefficients

The SST retrieval method should follow that described by Merchant et al (1999), and outlined in this section. In the case of the linear retrieval, the SST estimate, $\hat{x}$, is formed from a weighted combination of BTs. The SST retrieval coefficients define the weighting applied to each BT. The SST retrieval is defined in matrix-vector notation in Eq. 3.5: all vectors are column vectors and appear as lower case; all matrices appear in uppercase; and the transpose operator is the superscript T.

$$\hat{x} = a_0 + \mathbf{a}^T \mathbf{y} \qquad\qquad 3.5$$

Here a_o is the offset coefficient, and $\mathbf{a}^T = [a_1, \ldots, a_n]$ is a vector of n weighting coefficients that each multiply one of the n BTs in the observation vector $\mathbf{y}$. These observations may consist of infrared observations at different wavelengths and/or view angles. The superscript, ^{T}, indicates the transpose of the vector, $\mathbf{a}$.

The offset and weighting coefficients are found using least squares minimization techniques. These minimize the mean square difference between the "true" SST input to the RTM and the "retrieved" SST given by Eq. 3.5, for the population of atmospheric and surface states and associated RTM BTs outlined in §3.1.1. The weights and offset term are given by the formulas:

$$\mathbf{a} = \left(\mathbf{S}_{yy} + \mathbf{S}_{\varepsilon}\right)^{-1} \mathbf{s}_{xy} \qquad\qquad 3.6$$

$$a_0 = \bar{x} - \mathbf{a}^T \bar{\mathbf{y}} \qquad\qquad 3.7$$

where x is the "true" SST associated with a given set of simulated BTs ($\mathbf{y}$); $\mathbf{S}_{yy}$ is the covariance matrix of observations; $\mathbf{S}_{\varepsilon}$ is the covariance matrix proposed (Zavody et al, 1995) to address the noise equivalent differential temperature; and $\mathbf{s}_{xy}$ is the covariance vector of SST and observations. Bars above variables indicate mean values. The covariance matrix of the observations, $\mathbf{S}_{yy}$ is defined as:

$$\mathbf{S}_{yy} = \overline{\mathbf{y}\mathbf{y}^{T}} - \overline{\mathbf{y}}\,\overline{\mathbf{y}}^{T} \qquad\qquad 3.8$$

and the covariance vector of SST and observations, s_{xy}, is given by:

$$\mathbf{s}_{xy} = \overline{x\mathbf{y}^{T}} - \overline{x}\,\overline{\mathbf{y}}^{T} \qquad\qquad 3.9$$

The covariance matrix describing the BTs, S_{ε}, can be taken to be a diagonal (i.e. noise is assumed independent between channels and forward model noise is neglected). Synthetic noise should be added to S_{ε} (as done by Zavody, 1995). This should be in the form of mean NEΔT values for each channel, squared and added to the diagonal elements of S_{ε}.

3.1.2.2 Channel/view combinations

SST retrieval coefficients must be defined, as in §3.1.2.1, for each combination of instrument channels and across-track/forward views that is to be used to estimate SSTs. Four channel/view combinations are used. These are:

- N2 – across-track single-view day-time retrieval (3.7 µm and along-track view are unused)

- N3 – across-track single-view night-time (along-track view unused)

- D2 – dual view day-time (3.7 µm unused)

- D3 – dual view night-time (all channels used)

This notation will be used throughout the remainder of this document. In general, dual view retrievals are preferred as they are more accurate and robust to stratospheric aerosol. Differences between retrievals made using the four algorithms are indicative of a problem with either the cloud screening or SST retrieval algorithms, e.g. undetected cloud in the forward view will result in incorrect dual view retrievals, while co-incident single-view retrievals are unaffected.

3.1.2.3 Requirements for coefficients

In order to limit the contribution to retrieval errors from the mis-specification of retrieval coefficients to << 0.1 K, weighting coefficients must be defined to a precision of five decimal places with uncertainty permissible in the last digit, as discussed by Merchant and Le Borgne (2004). This level of precision assumes BTs and SSTs are expressed in kelvin. If these are expressed in degrees Celsius, then only precision to four decimal places is required to achieve

the same SST precision, since the relevant temperatures are an order of magnitude smaller than the corresponding temperatures in kelvin.

Any error in the offset coefficient, a_O, translates directly as an error (global bias) in the retrieved SST. Therefore, to meet the accuracy target of 0.1 K the offset coefficient must be specified to within a tenth of a kelvin, and therefore two decimal places are required.

3.1.2.4 Viewing geometry considerations

The variations in viewing geometry across the satellite swath and the differences in these variations between across-track and along-track views must be incorporated into the SST retrieval coefficients. In doing so, it is necessary to consider the following points about the viewing geometry and its relationship to the retrieval coefficients.

Satellite zenith angles may not be a fixed function of the distance (in pixels) from the centre of the satellite swath.

The swath may be asymmetric - i.e. zenith angles are different at each edge (depending on satellite roll)

The retrieval coefficients are best chosen to be linear with path length (secant of view zenith angle)

Figure 7 (left) shows the actual satellite path lengths for 32 positions spaced evenly across the swath for one complete orbit of ATSR-2 compared to a viewing geometry assuming a standard symmetrical swath (implicit in the operational across-track scheme for ATSR SSTs). Figure 7 (right) shows the effect of these angle variations on the retrieved SST, for D3 retrievals. The local biases of up to 0.2 K from the assumed viewing geometry can be corrected using a more refined approach. A look-up-table of SST retrieval coefficients must be calculated for a range of viewing angles, for both single and dual-view retrievals. As a minimum, a look-up-table containing coefficients for 30 across-track/along-track view combinations (5 across-track angles by 3 along-track angles) is required for dual view retrievals. These coefficients will then be bi-linearly interpolated to the viewing geometry of the target pixel. Provisional sets of across-track and along-track view angles for which the look-up-table of coefficients are to be prepared for SLSTR are given in Table 5. This table needs to be refined once the viewing geometry in design and in flight is finally specified.
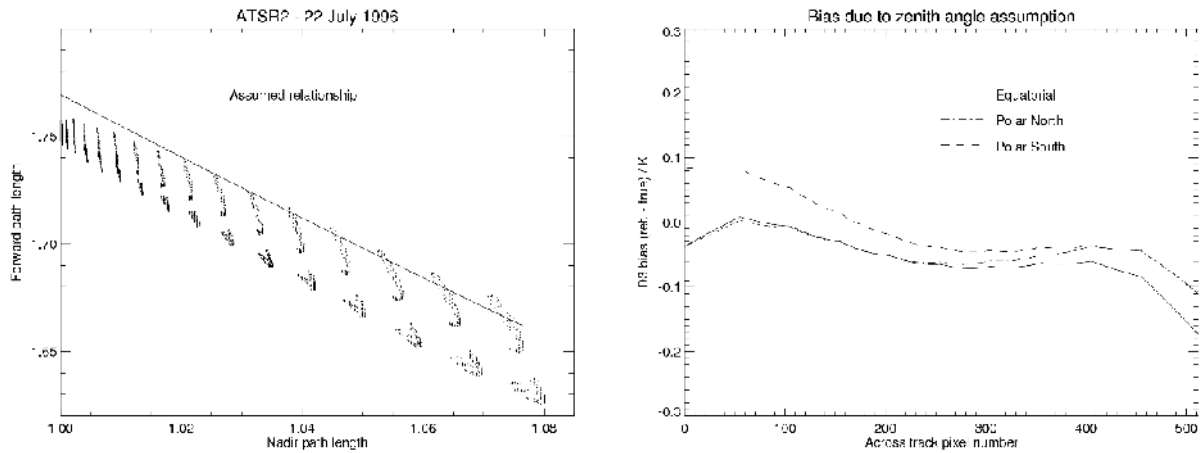
Figure 7. Effect of zenith angle assumptions. Left: Actual and assumed path lengths. Right: SST bias due to zenith angle assumption for three along track positions in satellite orbit. Biases calculated using the same simulations as used for generating coefficients.

View	Path lengths (sec(satellite zenith angle))
Across-track single-view	*1.0, 1.1, 1.2, 1.3, 1.4, 1.5, 1.6, 1.7, 1.8, 1.9, 2.0*
Across-track dual-view	*1.000, 1.015, 1.030, 1.045, 1.060, 1.075, 1.090, 1.105, 1.130, 1.145, 1.160*
Along-track	*1.70, 1.74, 1.78*

Table 5. Provisionally recommended viewing angles (defined as path lengths) for which a look-up-table of SST retrieval coefficients should be calculated.

3.1.2.5 Water vapour banding

Retrieval coefficients should also be defined as a function water vapour. It is recommended that coefficients are defined for overlapping bands of total column water vapour (TCWV). Coefficients should be defined for each water vapour band, using only the profiles from the profile data set (§3.1.1.5) where TCWV is within the specified range of the band. A suitable range for each TCWV band is 10 kg m^{-2}, with a 5 km m^{-2} overlap between bands (e.g. [0,5], [0,10], [5,15].....[55,65]). The use of overlapping bands prevents discontinuities in SST between bands. To avoid extrapolation errors, the distribution of TCWV in each band needs to have a mean value equal to the band centre. A simple linear interpolation between coefficients of adjacent TCWV bands, based on the NWP TCWV value, should be used in SST retrievals. The benefits of using water-vapour banded coefficients are illustrated in

Figure 8. Using water vapour banded coefficients removes significant trends in bias with TCWV and also reduces the SD.
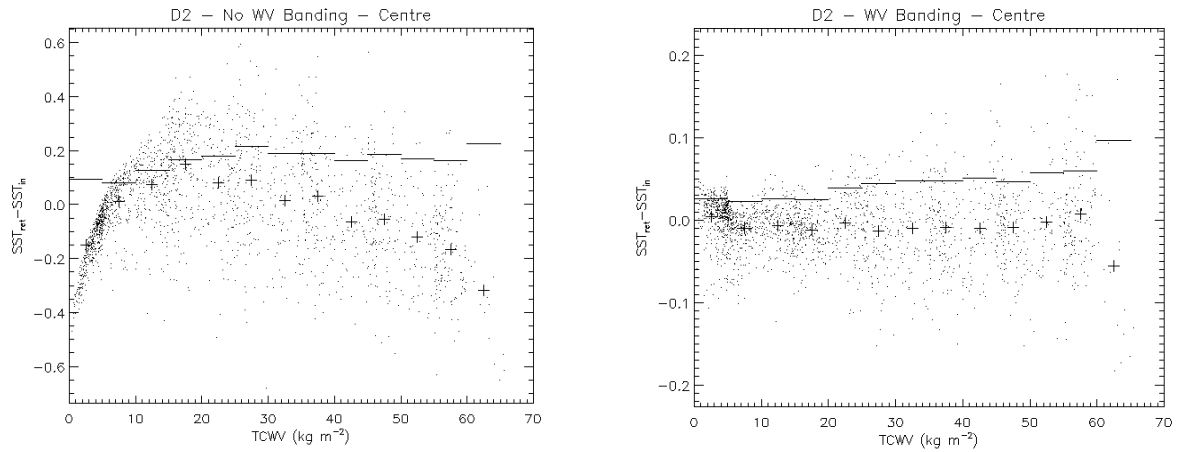

Figure 8. Effect of using water vapour banded coefficients on retrieval error for D2 retrievals. Bias (+) and SD (-) are calculated for TCWV bands of size 5 kg m^{-2}. Note the difference in scales of the vertical axes.

3.1.2.6 Robustness to aerosol

Both tropospheric and stratospheric aerosol are considered in the forward model, as described in §3.1.1.4 and §3.1.1.5. In addition to this, the SST retrieval coefficients must be robust to stratospheric aerosol loading events (major volcanic eruptions). Although there is no significant stratospheric aerosol loading at time of writing, retrieval coefficients robust to stratospheric aerosol should be used, in order to maintain an SST time series consistent seamlessly in the face of any future eruption.

SST retrieval coefficients can be made robust to stratospheric aerosol events through an extension to the formulisation for the retrieval coefficients given in §3.1.2.1 (Eqns. 3.6 and 3.7), as described by Merchant et al (1999) and outlined in this section.

Adding stratospheric aerosol changes the BTs in the observation vector, **y**, as follows.

$$\mathbf{y} = \mathbf{y} + c\delta\mathbf{k} \qquad\qquad\qquad \textbf{3.10}$$

where **k** is a vector representing the mode of variation for the aerosol type, δ is the aerosol optical depth, and c is nearly constant (it has a weak dependence on upwelling radiance). Aerosol modes, **k**, are represented in the form of BTs corresponding to differences between aerosol-free atmospheres and atmospheres with different aerosol loadings. Aerosol modes of this form can be calculated using a suitable RTM and scattering model, as described in §3.1.1. This should be done for a suitable set of globally representative atmospheric profiles (such as that described in §3.1.1.5) and for a range of viewing geometries (e.g. Table 5).

The change in the SST estimate associated with stratospheric aerosol can be seen by substituting Eq. 3.10 into Eq. 3.10 and is equal to $c\delta\mathbf{a}^T\mathbf{k}$. The requirement for an SST retrieval to be unaffected by stratospheric aerosol is therefore that:

$$\mathbf{a}^T\mathbf{k} = 0 \tag{3.11}$$

Equation 3.11 defines the property of "aerosol robustness", and the methods used to incorporate this property in SST retrieval coefficients is described in detail by Merchant et al (1999). The linear constraint, given by Eq. 3.11 must be satisfied for every stratospheric aerosol mode required. Merchant et al (1999) show that by putting the required modes $\mathbf{k}$ into a matrix of column vectors $\mathbf{K}$, the expression for aerosol robust coefficients can be written as:

$$\mathbf{a} = \mathbf{S}_{yy}'^{-1}\left[\mathbf{s}_{xy} - \mathbf{K}\left(\mathbf{K}^T\mathbf{S}_{yy}'^{-1}\mathbf{K}\right)^{-1}\left(\mathbf{K}^T\mathbf{S}_{yy}'^{-1}\mathbf{s}_{xy}\right)\right] \tag{3.12}$$

where $\mathbf{S}_{yy}'^{-1} = \mathbf{S}_{yy} + \mathbf{S}_{\varepsilon}$. The benefit of full orthogonality to the required aerosol modes is accompanied by a cost: an increase in the SST retrieval error variance (that is, the expectation of $\left[\{\hat{x} - x\} - \overline{\{\hat{x} - x\}}\right]^2$) under aerosol-free conditions, given by:

$$\Delta s_{\hat{x}} = \left(\mathbf{K}^T\mathbf{S}_{yy}'^{-1}\mathbf{s}_{xy}\right)^T\left(\mathbf{K}^T\mathbf{S}_{yy}'^{-1}\mathbf{K}\right)^{-1}\left(\mathbf{K}^T\mathbf{S}_{yy}'^{-1}\mathbf{s}_{xy}\right) \tag{3.13}$$

This increase in SST retrieval error variance $\Delta s_{\hat{x}}$ must be kept small for aerosol-robust coefficients to be useful. In general, $\Delta s_{\hat{x}}$ increases (1) with increases in the number of aerosol modes in $\mathbf{K}$, and (2) the closer the aerosol modes are to $\partial\mathbf{y}/\partial\mathbf{x}$ (i.e. the mode of variation associated with changes in true SST). Two degrees of freedom are required to retrieve SST in the absence of significant aerosol with a reasonable degree of atmospheric correction. This coupled with the behaviour of $\Delta s_{\hat{x}}$ limits the number of and which aerosol types the retrieval can be made robust to, depending on the channel/view combinations used in the retrieval. For example, D2 retrieval s (4 BTs) can only be made robust to one or two aerosol modes. Coefficients for the D2 retrieval that are robust to three aerosol types will suffer an unacceptable increase in retrieval variance.

The recommended equations for calculating the coefficients for each combination of channels and viewing geometry are given in Table 6. To provide continuity with the ATSR series of instruments, it is recommended that dual-view retrieval schemes using two and three spectral channels are developed, and that these retrieval coefficients are robust to background stratospheric aerosol. The aerosol modes for these background conditions, as used for AATSR in the ARC project (Merchant et al, 2008) are given in Table 7. Their equivalents must be calculated for SLSTR SRFs once these are defined.

	Eq. 3.6/3.7	Eq. 3.12
N2	Y	
N3	Y	
N3R		Y
D2		Y
D3		Y

Table 6. Equations which should (Y) be used for calculating coefficients for each retrieval type. The A3R retrieval is proposed as a "reserve" set of coefficients that may be calculated for use in the event of a significant future volcanic eruption.

	3.7 μm	11 μm	12 μm
Across-track	-0.307	-0.382	-0.219
Along-track	-0.487	-0.599	-0.341

Table 7. Normalised relative sensitivity to stratospheric for AATSR as used in the ARC project (Merchant et al, 2008). Equivalents for each zenith angle in Table 5 will be required for SLSTR.

3.1.3   Treatment of Errors

3.1.3.1 Introduction

All SST retrievals will have an associated error estimate. Appropriate consideration and incorporation of errors from all possible sources is important for any SST retrieval scheme. Errors are typically split into two broad categories: systematic and random. Systematic errors are described in terms of bias and give a measure of the accuracy of the retrieval. This is normally represented by the mean difference between retrieved values and "truth" data (e.g.

in situ buoy measurements). Random errors are described in terms of scatter and provide an estimate of the precision of the retrieval. The standard deviation (SD) of the differences between retrieved and "truth" data are commonly used to represent this error type. Although these basic categorisations may be used to provide an overall picture of the errors in a retrieval scheme, error characteristics are in reality more complex, as discussed below.

3.1.3.2 Systematic Errors

Forward modelling errors

Systematic errors are introduced to the retrieval through the forward model, specified in 3.1.1, that is used to simulate radiances, $\mathbf{y}$, where:

$$\mathbf{y} = F(\mathbf{x},\mathbf{b}) + \varepsilon_F \qquad\qquad 3.14$$

Here, F represents the function of the RTM, and ε_F the radiative transfer model error. The surface and atmospheric state are described by $\mathbf{x}$, while $\mathbf{b}$ incorporates other model parameters such as spectroscopic data and sensor characterisation. The RTM error, ε_F, represents the departure of the simulation from what would really be observed by a sensor observing the situation described by $\mathbf{x}$ and $\mathbf{b}$, but it does not account for errors due to systematic differences between state vectors and reality or errors in the model parameters. Including these errors, the full forward model error can described as:

$$\varepsilon_y = \varepsilon_F + \frac{\partial F}{\partial \mathbf{x}}\varepsilon_x + \frac{\partial F}{\partial \mathbf{b}}\varepsilon_b \qquad\qquad 3.15$$

where the subscripts of ε define the parameter in error. As discussed by Merchant and Le Borgne (2004), any or all of the terms in Eq. 3.15 can be significant in the context of SST retrievals.

The forward model error, ε_y, propagates through into the SST retrieval error. Contributions to the error from forward model parameters can be isolated by performing identical radiative transfer simulations, except for perturbed values of the parameters of interest. Defining $\mathbf{y}_p$ as the BTs simulated after a perturbation, Δb, of parameter, b, of the forward model, the resulting error in BT from a parameter error of size Δb can be defined as:

$$\mathbf{e}_b = \mathbf{y} - \mathbf{y}_P \cong \frac{\partial F}{\partial b}\Delta b \qquad\qquad 3.16$$

Substituting this into the retrieval equation (Eq. 3.5) reveals that the SST error associated with the parameter error, Δb, is given by:

$$\mathbf{e}_{SST} = \mathbf{a}^T \mathbf{e}_b \qquad\qquad 3.17$$

Eqs. 3.16 and 3.17 should be evaluated at the stage of coefficient generation for a number of model parameters using methods such as those of Merchant and Le Borgne (2004). The model parameters for which error propagation should be evaluated and an example of their impact on ATSR-2 retrievals are given in Table 8.

Model Parameter	Example Perturbation	ΔSST retrieval	
		Bias (K)	ΔSD (%)
Sea surface emissivity	Increase by 0.001 (approximate uncertainty estimate for emissivity)	-0.05	0.4
Trace gas profiles	Change in concentrations from 1999 to 1991 levels (for SLSTR, recommend trace gas levels for 2014 and projected levels for 2025).	-0.03	0.03
Water vapour continuum parameterization	Different parameterizations, e.g. CKD 2.2.2 and MT_CKD (see http://www.rtweb.aer.com/), as appropriate at time of implementation	0.01	0.08
Humidity profile	Reduce upper-tropospheric humidity by 15% (systematic error in UTH of this magnitude in NWP profiles is conceivable)	-0.04	6.8
Instrument SRF	Random changes of to the normalized SRF within the SRF uncertainty	-0.12	4.4

Table 8. Model parameters (and example perturbations) for which Eqs. 3.16 and 3.17 should be evaluated. Example perturbations and resulting errors in SST taken from Merchant and Le Borgne (2004).

Other systematic errors

There is also a contribution to the overall systematic error from the satellite calibration. The contribution from satellite calibration errors must be assessed by propagating calibration uncertainties through retrieval coefficients.

Additional errors caused by stratospheric volcanic aerosol may also need to be considered, in the event of significant volcanic activity during the instrument lifetime. Such errors can be considered as systematic, asymmetric errors. Stratospheric volcanic aerosols have life-times longer than synoptic time scales and affect regions on up to hemispheric space scales. Provided aerosol robust coefficients have been calculated (§3.1.2.6) then the effect of any future stratospheric aerosol is already addressed for dual-view retrievals. However, single-view coefficients cannot so readily be made rigorously aerosol robust (Merchant and Le Borgne, 2001) and therefore the N3R coefficients should not be used except in the situation of volcanic aerosol being present.

3.1.3.3 Random Errors

Radiometric noise

The radiometric noise in the sensors depends on the scene radiance (or BT) and the temperature of the detector. Radiometric noise expressed as a noise equivalent differential temperature will be available to the SST retrieval within the processing chain.

The radiometric noise propagates through the SST retrieval coefficients, allowing an overall estimate of the radiometric noise in the retrieval to be obtained using Eq. 3.18.

$$\varepsilon_{rad} = \sqrt{a_1^2 \varepsilon_1^2 + a_2^2 \varepsilon_2^2 + ... + a_n^2 \varepsilon_n^2} \qquad \textbf{3.18}$$

Here a_1 to a_n represent the SST retrieval coefficients for channel/viewing angle combinations 1 to n, and ε_1 to ε_n represent the corresponding noise equivalent delta temperatures (NEΔT) for the given channels at the scene temperature.

Pseudo-random – symmetric

In addition to the random error contribution from radiometric noise, there are other error contributions that may appear random but are not in fact random if fully understood. Such errors can be classed as pseudo-random and can be split into two subcategories: symmetric and asymmetric. Errors falling into each category are described in this and the following sections.

Symmetric pseudo-random retrieval errors are categorised as prior and nonlinearity errors in Merchant et al (2005), and are respectively; errors arising through systematic differences between the prior state (mean of states used in the regression database) and states for a given region and/or season; and errors arising from nonlinearity in the equations of radiative transfer.

Prior errors are correlated up to synoptic scales in space and time, but appear as scatter in a validation over a sufficiently large region and period. As the variability of prior error is predominantly due to variability in atmospheric water vapour (having used TCWV-banded coefficients), their magnitude can be estimated as a function of TCWV.

An estimate of the error associated with water vapour variability should be obtained through simulated SST retrievals for the instrument, using NWP data. A diverse set of atmospheric profiles from NWP (e.g. §3.1.1.5) should be used to provide a set of TCWV values and corresponding simulated BTs. From these BTs, SST estimates may be calculated for each channel/view combination (N2, N3, N3R, D2, D3) using retrieval coefficients generated as described in §3.1.2. The error associated with water vapour variability may then be estimated

through analysis of the standard deviation of the $SST_{retrieval}$-SST_{NWP} for different bands of TCWV.

An initial estimate of the contribution to the retrieval error from water vapour variability may be taken from analysis of simulated AATSR retrievals. For AATSR, using TCWV-banded coefficients, the contribution (SD) to the retrieval error can be described by a linear function of TCWV for each retrieval type. The gradient and intercept of each of these functions are given in Table 9. This error is observed to increase significantly with increasing TCWV for twin-channel retrievals (N2 and D2) but may be considered as a constant for three-channel retrievals. It is assumed here that N3R behaves like N3. The functions given in Table 9 are for centre swath viewing geometry. For AATSR, error associated with water vapour variability is observed to be approximately linear with increasing path lengths.

	N2	N3	D2	D3	N3R
m (K kg^{-1} m^2)	$0.01\sec(\theta)$	0.00	0.002	0.00	0.00
C (K)	0.07	0.07	0.07	0.07	0.07

Table 9. Approximate coefficients of straight line equations describing the pseudo-random symmetric contribution to retrieval error as a function of TCWV for AATSR.

The coefficients above found for AATSR in simulation should be revised for SLSTR once the SLSTR SRF are defined, as part of the coefficient definition process. This will then define the coefficients in the following model for symmetric pseudo-random error:

$$\varepsilon_{PR-symmetric} = C + mw \qquad\qquad 3.19$$

where C and m are retrieval-type specific coefficients and w is the prior estimate of total column water vapour from the L1B product (interpolated to the pixel from the nearest oceanic tie points).

Pseudo-random – asymmetric

Another source of pseudo-random error in the SST retrievals takes the form of cloud contamination in the channel brightness temperatures. This contamination may be a result of either residual cloud in view or reflections from clouds (in the along-track view). The contribution to the overall retrieval error from this source may be determined empirically, post-launch, through comparisons of retrieved SSTs (SST_{ret}) with in-situ observations (SST_{buoy}) for different levels of cloud cover in neighbouring pixels. Comparison of the root-

40

mean-square deviation (RMSD) of the SST difference ($\Delta SST = SST_{ret}\text{-}SST_{buoy}$), between clear-sky conditions and cases with differing numbers of adjacent cloudy pixels, yields an estimate of the error contribution as a function of cloud cover in adjacent pixels. Such analysis should be performed for each retrieval type, but can only be done in practice in flight for a given cloud detection scheme in practical operation.

The form of the contribution can be obtained from experience with from AATSR validation data. Calculating the RMSD of ΔSST, relative to that for clear-sky conditions, for increasing numbers of adjacent cloudy pixels, enables the error contribution to be defined as a function of cloud cover in adjacent pixels. For all retrieval types, the relative RMSD (to the clear-sky case) may be described as a linear function of the number of adjacent pixels contained cloud. The gradient and intercept of this function were found (using operational cloud screening) to be approximately the same for each retrieval type, and are given in Table 10, for AATSR.

	N2	N3	D2	D3	N3R
m [K]	0.068	0.068	0.057	0.073	n/a
C [K]	0.0	0.0	0.0	0.0	n/a

Table 10. Coefficients of straight line equations describing the contribution to retrieval error as a function of the number of adjacent pixels containing cloud for AATSR (no N3R has been made for AATSR).

Since this approach is empirically based, the assumption for SLSTR at launch can only be an approximate model based on the above experience, with refinements to be obtained from validation activities during operations. An appropriate at-launch assumption (assuming comparable sensitivity of cloud screening for SLSTR as AATSR) appears to be

$$\varepsilon_{PR\text{-}asymmetric} = 0.0 + 0.07\frac{9-n_c}{8}$$ 3.20

independently of the retrieval type, where n_c is the number of clear pixels in the 3 x 3 pixel box centred on the current pixel.

Combining random errors

The (pseudo) random errors discussed in §3.1.3.3 are combined to provide an overall estimate of the retrieval error using (treating the asymmetric error as if it were zero mean):

$$\varepsilon_{totalrandom} = \sqrt{\varepsilon_{rad}^2 + \varepsilon_{PR-sym}^2 + \varepsilon_{PR-asym}^2}$$ 3.21

This is the pixel level error estimate to be associated with each SST-type for each pixel in full resolution products.

3.1.3.4 Other errors

Errors resulting from sampling should also be considered. Incorrect cloud screening is one example of such errors. Consequently, the limitations of the cloud screening method used must be understood and the potential error contribution assessed. Additional errors may arise from both cloudy contaminated scenes being flagged as clear and from valid clear-sky scenes being flagged as cloudy. The former of these cases should be dealt with, at least partially, through the estimate of cloud contaminant error outlined in §3.1.3.3. The second case, where valid SSTs are flagged as cloud, is more likely to eliminate cold than warm features in SST. In doing so, warm biases may be introduced into averaged SST products. As errors arising from incorrect cloud screening are dependent on the cloud screening methods used, these errors must be assessed during the mission.

Another source of sampling error arises from the nature of the Sentinel orbit and swath. As a sun-synchronous polar orbiting satellite, observations are made at a fixed local time on each overpass. Consequently diurnal variations in SST cannot be fully captured and diurnal variations in cloud cover may result in consistently low SST coverage for some regions.

However, the above errors are of a different type to the error estimated with Equation 3.21, which is an appropriate error for the SST estimate taken for what it is: an observation of SST at a particular location and instant.

Sampling errors within areas must be considered when creating and analysing spatially and temporally averaged SST products, as in the following section.

3.1.4   Averaged Products

Spatially and temporally averaged SST products should be generated for each SST retrieval type independently. Averaging should be performed using the retrieved SST values on the Sentinel footprint scale (rather than calculating SSTs from averaged channel BTs). Only pixels with valid SST retrievals for the specific retrieval type should be used to produce the averaged SST product for that retrieval type, using Eq. 3.22.

$$SST_{i,j} = \frac{\sum G_{k,l}\left(SST_{k,l}\right)}{\sum G_{k,l}}$$ 3.22

Here i, j represent the coordinates of the cell in the averaged product, k, l represent the pixel coordinates within the cell of dimension N. $G_{k,l}$ is a cloud-screening operator that takes a value of

   0 when the pixel, k, l is cloudy in any of the views used for the current retrieval type

   1 when the pixel is cloud-free.

Eq. 3. should be used to calculate averaged SST products for each retrieval scheme independently. Single-view SSTs for a given cell may be based on a different sample from any dual-view SST for that cell, if the cloud mask for the along-track view differs from the across-track view (which in general it does).

The definitions of the grids and cells to be used for SLSTR is independent of the above method, and is specified elsewhere.

The error estimate associated with $SST_{i,j}$ needs to take into account the distinction between random and pseudo-random error, and uncertainty from sub-sampling within the grid cell. It is assumed that radiometric errors are completely uncorrelated between pixels in the cell (true except for cosmetic fill pixels), while PR errors are assumed correlated across the cell (and therefore not reduced by averaging over pixels). The appropriate error estimate is therefore

$$\varepsilon_{i,j} = \sqrt{\frac{\sum G_{k,l}\left(\varepsilon_{rad,k,l}^{2} + \right)}{\left(\sum G_{k,l}\right)^{2}} + \frac{\sum G_{k,l}\left(\varepsilon_{PR-sym,k,l}^{2} + \varepsilon_{PR-asym,k,l}^{2}\right)}{\left(\sum G_{k,l}\right)} + \frac{\left(N - \sum G_{k,l}\right)\hat{V}_{SST,i,j}}{N-1}}$$

$$\hat{V}_{SST,i,j} = \frac{1}{\left(\sum G_{k,l}\right)-1}\sum\left(G_{k,l}x_{k,l} - \frac{\sum(G_{k,l}x_{k,l})}{\sum G_{k,l}}\right)^{2}; \quad \hat{V}_{SST,i,j} \geq V_{\min} \text{ if } \sum G_{k,l} < f_{\min}N$$

3.23

where the first two terms on the right follow directly by analogy with Equation 3.22 under the assumptions about correlations of errors with the cells. The final term represents the uncertainty in the cell average from sub-sampling, i.e., from the fact that SSTs under cloud pixels are not included, and the unknown SSTs for these pixels are therefore excluded from the cell average. It has the form of an estimate (indicated by the hat symbol) of the true variance of SST in the cell, $V_{SST,i,j}$ scaled by a fraction related to the proportion of the N pixels within the cell boundary that are included in the cell SST average. The justification for this model of sampling error is straight-forward: if only one pixel contributes to the cell average SST, the uncertainty from this sampling effect is the full variance of SST in the cell (as perceived at the SLSTR spatial resolution); if all pixels are clear, the sampling uncertainty is zero. The problem is then to find an estimate of $V_{SST,i,j}$ The options are (i) try to estimate it

from the observed data, or (ii) define an external reference (from a climatology of variability at an appropriate resolution for the grid-cells required). Where the grid cell is relatively completely observed, (i) is clearly preferable; however, if relatively few or one pixels are clear within the cell, such an estimate of $V_{SST,i,j}$ becomes highly uncertain or undefined. The second option is complex to define, being a function of observation resolution, grid cell size, location and seasonality. In the equation above, the option (i) is therefore assumed and the expression for the variance estimate is given. However, for the case where the number of clear pixels is 1 (variance undefined) or less than a fraction f_{min} of the cell (for which the variance estimate is particularly unreliable in the face of spatial correlations within the cell area), a minimum value, V_{min} should be imposed. The recommendation is $V_{min} = 0.1^2 \text{ K}^2$ and $f_{min} = 0.2$.

3.1.5 Full resolution L2P

A broad community of users will draw on full resolution L2P as their mode of use of SLSTR SSTs. There will be a single L2P product. The principal fields to do directly with SST are: SST estimate, SST bias estimate, single-sensor error statistic, quality flag.

In turn, these will be provided as follows:

SST estimate: of the one-to-four SST types available for a given pixel, one will be chosen as the L2P SST estimate; moreover, as an extra processing step, atmospheric correction smoothing will be applied to reduce noise in this SST estimate (see discussion below)

SST bias estimate: no at-launch value for this can be provided (other than zero) since the SST coefficients are intended to be zero-bias; actual biases must be assessed in validation and provision made for updating these during operations

SSES:

at launch, the uncertainty SSES will be the error estimate for the pixel/SST-type, modified for the noise reduction of atmospheric smoothing; the bias SSES will be set to zero or fill

the GHRSST definition for L2P products are based on validation statistics relative to drifting buoys; to comply with the GHRSST definition, therefore, some estimate for empirical SSES will need to be commissioned, but this is beyond the scope of the present document;

once a compliant SSES is available, the value from the comprehensive error model defined here for SLSTR should then be replaced with this empirical SSES; the uncertainty estimate from the error model value will be present as an experimental field (for which there is provision in L2P format)

quality flag: this is will be defined in the ATBD for cloud detection, since it is an indicator of degree of confidence in the assessment of a given pixel as clear

Experimental fields are available to be populated:

the uncertainty estimate from the error model

SSTs of all types available for that pixel (supplementing the selected SST for the main SST record)

each brightness temperature

the noise equivalent differential temperature corresponding to each brightness temperature

Choice of SST

Two approaches to choice of SST retrieval can be envisaged: a hierarchy of preference for different SST types; or, selection based on the least error estimate in the error model. Were it guaranteed that SST types would have small biases (<0.1 K) relative to each other, the latter would be natural. But since operational algorithms for ATSR series instruments have historically had relative biases ~0.2 K, it would not be ideal to risk a situation where two SST types were giving comparable error estimates and therefore there was random alternation of SST type between adjacent pixels. (Although, once appropriate SST bias estimates are available, this could stop being an issue.)

It is therefore decided that the choice of SST be based on a hierarchy of preference.

1. Normal conditions

Normal conditions impies: absence of above-background volcanic aerosol in stratosphere, no suspicion of Desert Dust, the order of preference (most to least preferred) will be:

D3 – N3 – D2 – N2   if solar zenith angle > 90°

D2 – N2   if solar zenith angle <= 90°

2. Desert Dust conditions

It is beyond the scope of this ATBD to specify a system for identification of desert dust aerosol in the atmosphere. Detection of desert dust as a distinct class from clear-sky and cloud is also not likely to be available in the initial cloud detection scheme for SLSTR. However, research (Merchant et al, 2006) has demonstrated the usefulness of detecting desert dust to inform SST retrieval strategy suggests, so the possibility of such information being available and used should be planned for.

Under conditions of no-stratospheric aerosol but where Desert Dust is suspected (by means not yet defined), the order of preference will be:

D3 – D2 – N3 -- N2   if solar zenith angle > 90°

D2 – N2   if solar zenith angle <= 90°

3. Stratospheric aerosol conditions

Under conditions of stratospheric aerosol loading (irrespective of any other condition), the order of preference will be:

D3 – D2 – N3R   if solar zenith angle > 90°

D2   if solar zenith angle <= 90°

and thus N2 will not be included in L2P (because such retrievals are cannot be valid under aerosol conditions).

Atmospheric smoothing of SST for L2P

In AATSR, a technique of smoothing of the atmospheric correction is applied to reduce the noisy appearance of images. The assumption underlying this procedure is that "atmospheric correction" (i.e., SST minus BT in a selected channel) should be constant over some space scale. While this is usually reasonable, the underlying assumption is not true across fronts (where there is a step change in atmospheric correction) nor around major cloud systems (where there may be a "halo" of enhanced water vapour loading). Because in these latter circumstances, atmospheric correction smoothing introduces subtle biases, it has not been defined for the full resolution reference products above. However, many users are used to the smoother visual appearance of smoothed SST fields, and so it has been decided that smoothing will be appropriate for L2P distribution. We preserve the precedent from AATSR of smoothing over a 3 x 3 pixel kernel.

Let p be an index over the pixels within the 3 x 3 box, with q referring to the central (current) pixel. Let i be an index enumerating channel-view combinations, and let j indicate the channel-view combination that acts as the reference for the atmospheric correction. The reference will be the across-track 11 µm channel, unless there is reason to choose otherwise (e.g., if this channel turns out to be unusually noisy; thus the flexibility to specify an alternative reference channel should be built in to the processor).

The L2P SST with atmospheric correction smoothing is therefore:

$$SST_{L2P} = y_{q,j} + \left(\frac{\sum G_p \left(SST_p - y_{p,j} \right)}{\sum G_p} \right) \qquad \textbf{3.24}$$

Here, G_p takes 1 for those values of p for which a clear-sky SST of the same type as SST_q is available, and 0 otherwise.

Error estimate for L2P SST (SSES)

Because the smoothed atmospheric correction includes the SST for the central pixel itself, the effect on error of atmospheric correction smoothing is a little complicated. To derive the L2P SST error estimate, we use the nomenclature that e is a particular realisation of an error drawn from an error distribution of standard deviation ε. From the form of Equation 3.23 and using 3.19 it follows that the radiometric error in the L2P SST is

$$e_{rad-L2P} = e_{q,j} + \frac{\sum_p \left(G_p \sum_i a_i e_{p,i} \right)}{\sum_p G_p} - \frac{\sum_p \left(G_p e_{p,j} \right)}{\sum_p G_p}$$

This can be re-expressed using terms that are uncorrelated with each other on the right hand side, as follows:

$$e_{rad-L2P} = \left(1 + \frac{a_j - 1}{\sum_p G_p} \right) e_{q,j} + \frac{\sum_{p \neq q} \left(G_p \sum_{i \neq j} a_i e_{p,i} \right)}{\sum_p G_p} + \frac{\sum_{i \neq j} a_i e_{q,i}}{\sum_p G_p} + \frac{\sum_{p \neq q} G_p \left(a_j - 1 \right) e_{p,j}}{\sum_p G_p}$$

The expected mean square deviation of the above is the radiometric "error" in the L2P SST. Since the terms are uncorrelated above, this corresponds straightforwardly to

$$\varepsilon_{rad-L2P} = \sqrt{\left(1 + \frac{a_j - 1}{n_c}\right)^2 \varepsilon_j^2 + \frac{(n_c - 1)\sum\limits_{i \neq j} a_i^2 \varepsilon_i^2}{n_c^2} + \frac{\sum\limits_{i \neq j} a_i^2 \varepsilon_i^2}{n_c^2} + \frac{(n_c - 1)(a_j - 1)^2 \varepsilon_j^2}{n_c^2}}$$

using $n_c = \sum\limits_p G_p$. Thus the L2P radiometric error resolves finally to

$$\varepsilon_{rad-L2P} = \sqrt{\frac{n_c - 1 + a_j^2}{n_c} \varepsilon_j^2 + \frac{\sum\limits_{i \neq j} a_i^2 \varepsilon_i^2}{n_c}} = \sqrt{\frac{n_c - 1}{n_c} \varepsilon_j^2 + \frac{\varepsilon_{rad}^2}{n_c}} \qquad \textbf{3.25}$$

which can be seen to correctly revert to the same value (Eq 3.18) as the full resolution product if there is only the central pixel clear within the box (n_c=1).

The total error

$$\varepsilon_{L2P-SSES} = \sqrt{\varepsilon_{rad-L2P}^2 + \frac{\sum\limits_p G_p \left(\varepsilon_{PR-sym,p}^2 + \varepsilon_{PR-asym,p}^2\right)}{n_c}} \qquad \textbf{3.26}$$

is the radiometric error from 3.25 appropriately combined with the mean square pseudo-random errors across the 3 x 3 kernel.

`Practical considerations`

Use of single-view robust coefficients N3R

There is no automated means of identifying when to switch from N3 to N3R coefficients. Moreover, past volcanic aerosol outbreaks have shown significant periods of time (a few months) in which the presence of aerosol was confined zonally or to a single hemisphere, before distributing more evenly to all latitudes. Therefore, provision should be made for operator intervention to switch on "volcanic aerosol conditions" for a restricted range of latitudes, in the light of information available about the distribution of the plume. During the first few months of a large event, the latitude range to switch would probably need to be updated weekly. Switching implies: use of N3R rather than N3 in all products; re-ordering of the priority list for the L2P SST; and suppression of N2 in the L2P product.

Look up tables (LUTs)

The dimension of the LUTs for coefficients will be, as a minimum:

Number of detector combinations * number of across-track angles *

number of along-track angles * number of TCWV bands * number of coefficients

Provisionally, the dimensions will be as shown in Table 11 along with a sufficient procedure for interpolation.

	No. along	No. across	No. bands	No. coefficients	Interpolation required (geometric interpolations are all in secant($\setminus$), TCWV band interpolations/extrapolations are with respect to band centre values).
N2	0	11	8	3	Bi-linear interpolation with respect to across track path length and TCWV bands.
N3	0	11	8	4	As N2
N3R	0	11	8	4	As N2
D2	3	5	8	5	Bi-linear interpolation between neighbouring across/along-track pairs, and linear interpolation between TCWV bands.
D3	3	5	8	7	As D2

Table 11. Dimensions for different sorts of coefficients, and comments on a sufficient approach to interpolation.

"Nadir" only algorithms will require a dimension of 2 to account for each detector combination (one of two possible pairs). Dual algorithms will require additional dimensions of 2 x 2 to account for each possible pairing of detectors for the along-track and across-track observations.

Unforeseen circumstances could give rise to additional dimensions. For example, if a channel's noise level fluctuated significantly, a dimension accounting for such variations could be added.

Post-launch improvement of inter-algorithm consistency

Within the ARC project, the residual biases of order 0.2 K that remain between algorithms based on radiative transfer are reconciled by adjusting the offset coefficient for all elements of the algorithm LUT to be consistent in the mean with the SST obtained by a designated reference algorithm (Embury and Merchant, submitted 2010). For SLSTR, the reference algorithm should be D3, assuming nominal instrumental performance. It is recommended to commission an exercise to improve inter-algorithm consistency in the post-launch period, using this approach.

Summary of adjustable parameters

Stratospheric- aerosol-episode-flag   Usually not set; when set, must also set next two parameters

Southerly-extent-of-volcanic-aerosol   Manually updated during episodes, ignored at other times

Northerly-extent-of-volcanic-aerosol   Manually updated during episodes, ignored at other times

Minimum-sample-variance-for-low-n   Review outcomes for gridded products during cal-val

Fraction-clear-in-cell-below-which-minimum-sample-variance-is-imposed   As above

Pseudo-random-symmetric-algorithm-error-constant   Redefine along with any coefficient changes

Pseudo-random-symmetric-algorithm-error-slope   Redefine along with any coefficient changes

Pseudo-random-asymmetric-algorithm-error-constant   Empirical: re-evaluate during cal-val and along with any changes to cloud detection

Pseudo-random-asymmetric-algorithm-error-slope   As above

Single-sensor-error-statistic   Empirical: re-evaluate periodically (annually) through mission

ASSUMPTIONS AND LIMITATIONS

SST retrieval co-efficients are based on measured SRFs and assume the anticipated levels of NEdT.

4. VALIDATION

Methods are based on AATSR methods within ATSR Reanalysis for Climate project, which are validated in Embury et al (2012b).

5. UNCERTAINTY BUDGET

This is addressed within section 3.1.3.

6. EVOLUTION

The contents of this ARBD have been fully implement in the baseline. Adjsutable parameters that depend on post-launch validation and error analyses will need to be updated within the processing chain once these are available are listed in section 3.2.

7. REFERENCES

Blake, D., Methane, Nonmethane Hydrocarbons, Alkyl Nitrates, and Chlorinated Carbon Compounds including 3 Chlorofluorocarbons (CFC-11, CFC-12, and CFC-113) in Whole-air Samples, *Trends: A Compendium of Data on Global Change*, CDIAC, Oak Ridge National Laboratory, Oak Ridge, Tenn., U.S.A., 2005

Chevallier, F., Sampled databases of 60-level atmospheric profiles from the ECMWF analyses, *SAF Programme: Research Report No. 4*, EUMETSAT/ECMWF, 2001.

Clough, S.A., Iacono, M. J. and Moncet, J.L., Line-by-line calculation of atmospheric fluxes and cooling rates: Application to water vapor. *J. Geophys. Res.*, 97, 15,761-15,785, 1992.

Cox, .C. and Munk, W., Measurement of the roughness of the sea surface from photographs of the Sun's glitter, *J. Opt., Soc., Am.*, 44, 838-850, 1954.

Deshler, T., Hervig, M.E., Hofmann, D.J., Rosen, J.M., and Liley, J.B., Thirty years of in situ stratospheric aerosol size distribution measurements from Laramie, Wyoming (41°N), using balloon-borne instruments, *J. Geophys. Res.*, 108 (D5), AAC 4-1-4-13, 2003.

Downing, H.D. and Williams, D., Optical constants of water in the infrared. *Journal of Geophysical Research*, 80, 1656–1661, 1975.

Embury, O., C. J. Merchant and M. J. Filipiak (2012a), A Reprocessing for Climate of Sea Surface Temperature from the Along-Track Scanning Radiometers: Basis in Radiative Transfer, Rem. Sens. Env., pp32 - 46, DOI: 10.1016/j.rse.2010.10.016

Embury, O. and C. J. Merchant (2012), A Reprocessing for Climate of Sea Surface Temperature from the Along-Track Scanning Radiometers: A New Retrieval Scheme, Rem. Sens. Env., pp 47 - 61, DOI: 10.1016/j.rse.2010.11.020

Embury, O., C. J. Merchant and G. K. Corlett (2012b), A Reprocessing for Climate of Sea Surface Temperature from the Along-Track Scanning Radiometers: Initial validation, accounting for skin and diurnal variability, Rem. Sens. Env., pp62 - 78. DOI:10.1016/j.rse.2011.02.028

Harris, A.R., Saunders, M.A., Global validation of the along-track scanning radiometer against drifting buoys, *J. Geophys. Res.*, 101 (C5), 12127-12240, 1996.

Highwood, E. J., Haywood, J. M., Silverstone, M. D., Newman, S. M., and Taylor, J. P., Radiative properties and direct effect of Saharan dust measured by the C-130 aircraft during Saharan Dust Experiment (SHADE): 2. Terrestrial spectrum, *J. Geophys. Res.*, 108 (D18), 8578, doi:10.1029/2002JD002552, 2003.

Keeling, C.D., and Whorf, T.P., Atmospheric CO_2 records from sites in the SIO air sampling network, *Trends: A Compendium of Data on Global Change*, CDIAC, Oak Ridge National Laboratory, Oak Ridge, Tenn., U.S.A., 2005

Marmorino, G.O. and Smith, G.B., Bright and dark ocean whitecaps observed in the infrared. *Geophysical Research Letters*, 32, L11604, doi:10.1029/2005GL023176, 2005.

Masuda, K., Takashima, T. and Takayama, Y., 1988, Emissivity of pure and sea waters for the model sea surface in the infrared window region. *Remote Sensing of Environment*, 24, 313–329, 1998.

Masuda, K., Infrared sea surface emissivity including multiple reflection effect for isotropic Gaussian slope distribution model. *Remote Sensing of Environment*, 103, 488–496, 2006.

Matthiesen, S., and Merchant, C.J., Sea Surface Temperatures in Marginal Ice Zones: Final Report on Pathfinder Project, School of Geosciences, The University of Edinburgh, 2003.

Merchant, C. J., Harris, A.R., Murray, M.J., and Zavody, A.M., Toward the elimination of bias in satellite retrievals of sea surface temperature 1. Theory, modelling and interalgorithm comparison, *J. Geophys. Res.*, 104, 23565-23578, 1999.

Merchant, C. J. and Le Borgne, P., Designing OSI-SAF sea surface temperature retrievals to be robust to stratospheric aerosol, *Proceedings of the 2001 Meteorological Satellite Data User's Conference*, Antalya, Turkey, October 2001.

Merchant C J, Embury O, Le Borgne P and Bellec B (2006), Saharan dust in night-time thermal imagery: detection and reduction of related biases in retrieved sea surface temperature, Rem. Sens. Env., 104, 15-30.

Merchant, C. J. and Le Borgne, P., Retrieval of sea surface temperature from space, based on modelling of infrared radiative transfer: Capabilities and Limitations, *J. Atmos. And Oceanic Technology*, 21, 1734-1746, 2004.

Merchant C. J., Horrocks L. A., Eyre J. and O'Carroll A. G., Retrievals of sea surface temperature from infra-red imagery: origin and form of systematic errors, *Quart. J. Royal Met. Soc.*, 132, 1205-1223.

Merchant, C.J., Llewellyn-Jones, D., Saunders, R.W., Rayner, N.A., Kent, E.C., Old, C.P., Berry, D., Birks, A.R., Blackmore, T., Corlett, G.K., Embury, O., Jay, V.L., Kennedy, J., Mutlow, C.T., Nightingale, T.J., O'Carrol, A.G., Pritchard, M.J., Remedios, J.J., Tett, S., Deriving a sea surface temperature record suitable for climate change research from the along-track scanning radiometers, *Advances in Space Research*, 41, 1-11, 2008.

Newman, S.M., Smith, J.A., Glew, M.D., Rogers, S.M., and Taylor, J.P., Temperature and salinity dependence of sea surface emissivity, *Quart. J. Royal Met. Soc.*, 131, 2539-2557, 2005.

Pinkley, L.W., Sethna, P.P. and Williams, D., Optical constants of water in the infrared: Influence of temperature. *J. Opt. Soc. Am.*, 67, 494–499, 1977.

Salisbury, J.W. and D'Aria, D.M., Thermal infrared remote sensing of crude oil slicks. *Remote Sensing of Environment*, 45, 225–231, 1993.

Saunders, R., and Brunel, P., RTTOV_8_7 Users Guide, EUMETSAT, 2005

Santee, M. L., et al. (2007), Validation of the Aura Microwave Limb Sounder HNO3 measurements, J. Geophys. Res., 112, D24S40, doi:10.1029/2007JD008721

Stamnes, K., SC. Tsay, W. Wiscombe and K. Jayaweera, Numerically stable algorithm for discrete-ordinate-method radiative transfer in multiple scattering and emitting layered media, Appl Opt 27 (1988) (12), pp. 2502–2509.

Tisdale, R. T., Glandorf, D. L., Tolbert, M. A., and Toon, O. B., Infrared optical constants of low-temperature H_2SO_4 solutions representative of stratospheric sulfate aerosols, *J. Geophys. Res.*, 103(D19), 25,353–25,370, 1998.

Tobin, D., Strow, L.L., A compilation of first-order line-mixing coefficients for CO_2 Q-branches, *J. Quant. Spectrosc. Radiat. Transfer*, 52, 281, 1994.

Watts, P.D., Allen, M.R., and Nightingale, T.J., Wind effects on the sea surface emission and reflection for the Along Track Scanning Radiometer, *J. Atmos. And Oceanic Technology*, 13, 126-141, 1996.

Wu, X.Q. and Smith, W.L., Emissivity of rough sea surface for 8-13 µm:modelling and verification, *Applied Optics*, 36, 2609-2619, 1997.

Zavody, A.M., Mutlow, C.T., Llewellyn-Jones, D.T., A radiative transfer model for sea surface temperature retrieval for the along-track scanning radiometer, *J. Geophys. Res.*, 100, 937-952, 1995.